

This material has been copied  
under licence from CANCOPY.  
Resale or further copying of this material is  
strictly prohibited.

Le présent document a été reproduit  
avec l'autorisation de CANCOPY.

La revente ou la reproduction ultérieure  
de ce document sont strictement interdites.

A THEORETICAL INTERPRETATION OF THE  
PRESSURE-TUBE, HEAVY-WATER, ZERO-ENERGY  
EXPERIMENT IN DIMPLE

D. A. NEWMARCH  
ATOMIC ENERGY ESTABLISHMENT,  
WINFRITH, DORCHESTER, DORSET,  
UNITED KINGDOM

Abstract — Résumé — Аннотация — Resumen

A THEORETICAL INTERPRETATION OF THE PRESSURE-TUBE, HEAVY-WATER, ZERO-ENERGY EXPERIMENT IN DIMPLE. An analysis is made of the lattice physics measurements which were performed in DIMPLE during 1960-61 on pressure-tube, heavy-water cores with various "coolants" in the pressure tube. The experimental reactivities and reaction rates are compared with Carlson Sn and Monte Carlo calculations in order to reveal any discrepancies between experiment and basic theory.

Predictions of the Winfrith five-group scheme have also been compared with experiment on the one hand and the more sophisticated theories on the other. It is shown that agreement between this simple method and experiment is to some extent fortuitous and results from errors cancelling each other.

INTERPRÉTATION THÉORIQUE D'UNE EXPÉRIENCE FAITE AU MOYEN DU RÉACTEUR DIMPLE DE PUISSANCE ZÉRO, A EAU LOURDE ET A TUBES SOUS PRESSION. L'auteur donne le compte rendu des mesures de physique des réseaux auxquelles il a été procédé en 1960-61 dans des cœurs à eau lourde et à tubes sous pression du réacteur DIMPLE, avec divers «fluides de refroidissement» dans les tubes sous pression. Il compare les valeurs de la réactivité et de la vitesse de réaction obtenues par cette expérience avec les résultats du calcul (méthodes Carlson Sn et de Monte-Carlo), afin de repérer les discordances qu'il pourrait y avoir entre les résultats de l'expérience et ceux de la théorie fondamentale.

Il compare en outre les prévisions de la théorie à cinq groupes de Winfrith, d'une part avec l'expérience, d'autre part avec des théories plus élaborées. Il montre que la concordance entre les résultats de cette méthode simple et ceux de l'expérience est en partie fortuite et provient d'une compensation d'erreurs.

ТЕОРЕТИЧЕСКОЕ ИСТОЛКОВАНИЕ ЭКСПЕРИМЕНТА НУЛЕВОЙ МОЩНОСТИ С ТЯЖЕЛОЙ ВОДОЙ В ТРУБКАХ ПОД ДАВЛЕНИЕМ В РЕАКТОРЕ DIMPLE. Дается анализ физических измерений решетки, которые были проведены на реакторе DIMPLE в течение 1960 - 1961 годов по активным зонам с тяжелой водой в трубках под давлением с применением различных "теплоносителей" в трубках под давлением. Реактивность, определенная экспериментальным путем, и скорость реакции сравниваются с расчетами Карлсона и Монте-Карло для того, чтобы обнаружить расхождения между теорией и экспериментом.

Было проведено также сравнение предсказаний пятигрупповой схемы Уинфрита с данными опыта, с одной стороны, и с теоретическими данными - с другой. Указывается на то, что совпадение этого простого метода с опытом до некоторой степени случайно и что результаты ошибок исключают друг друга.

INTERPRETACIÓN TEÓRICA DE UN EXPERIMENTO EFECTUADO EN TUBOS DE PRESIÓN EN EL REACTOR DIMPLE, DE POTENCIA NULA Y AGUA PESADA. La memoria analiza las mediciones de física de los retículos que se realizaron en 1960 y 1961 en el reactor Dimple con cuerpos de reactores provistos de tubos de presión y agua pesada, empleando diversos «agentes refrigerantes» en los tubos de presión. Las reactividades experimentales y las velocidades de reacción se comparan con las calculadas por los métodos de Carlson Sn y de Montecarlo con miras a poner de manifiesto las discrepancias que pudieran existir entre los resultados experimentales y los de la teoría fundamental.

Las predicciones del esquema de Winfrith de cinco grupos se han comparado también con los datos experimentales y con otras teorías más complejas. Se comprobó que la concordancia entre este método sencillo y el experimento es en cierto modo casual y se debe a una compensación de errores.

## I. INTRODUCTION

### 1. Summary

This report gives a theoretical interpretation of the lattice physics measurements which were performed in the DIMPLE reactor at Harwell during 1960-1961. Bucklings and reaction rates were measured in these experiments, a full description of which is given by HYDER and HILBORN [1]. The lattice design of these cores is given in detail in section 2. Briefly they consist of fuel bundles, with various coolants, which are separated from the  $D_2O$  bulk moderator by a pressure tube, an air gap, and a calandria tube.

From the lattice physics point of view, these systems are complicated because of the large spectrum variations across the cell. The thermal spectrum is soft in the bulk moderator, while in the large fuel bundles the spectrum tends to take up the type of distribution characteristic of an infinite close-packed fuel bundle. It is necessary, therefore, to use more than one thermal group in the analysis. Above the fast-fission threshold, the flux shows a marked variation across the lattice cell. Below these energies, the fast flux shows little spatial variation. It is therefore essential to use at least two fast groups. Complications arise in the calculation of the resonance absorption: within the close-packed fuel bundles the fuel rods shield each other from the incoming current of resonance neutrons and therefore reduce the surface absorption effects; these shadowing factors are much reduced on the outside of the bundle. There are two demands made on the interpretation of experimental results. First, a comparatively simple theoretical model must be produced which can easily be used for surveys and preliminary design studies. Secondly, both the experimental results and the simple theory must be checked against more elaborate methods. The comparison of simple theory with the best theoretical methods enables the range of validity of the simple theory to be established; if this range is inadequate, modifications can be made. The comparison of experiment with the best theoretical methods, can bring new phenomena to light.

The simplest method used in this interpretation, is the Winfrith 5-group scheme, embodied in the SANDPIPER III and ARISTOS Mercury computer programmes. SANDPIPER III [2] generates cross-sections for three fast and two thermal groups; these are inputted directly into Aristos, without manual intervention, on either paper tape or punched cards. ARISTOS [3] is a 5-group diffusion theory code which calculates fine structure, reaction rates and reactivities. These two programmes are fast and easy to use. They do, however, introduce the errors inherent in diffusion theory; they also use the rather crude overlapping two thermal groups model. Since this work was started, the functions of SANDPIPER III and of ARISTOS have been combined in a single FORTRAN programme, METHUSELAH [16]. The physics of this programme is in some respects an improvement on that of the Mercury programmes, and METHUSELAH results are therefore compared with those from SANDPIPER/ARISTOS.

These two deficiencies, together with other approximations involved in the current versions of the codes, necessitate that the results should be corrected. The errors due to diffusion theory were corrected by a

comparison with 5-group Carlson calculations (see section 4), while the errors due to the use of two thermal groups were examined by a comparison with forty-group Carlson calculations spanning the thermal energy range (see section 5). Corrections are also made for (n, 2n) effects, end-plate effects, and leakage.

The corrected results enable one to determine whether there are any fundamental inconsistencies between theory and experiment. Also a comparison of the corrected results with the simple five-group results enables the validity of the ARISTOS/SANDPIPER scheme to be judged.

This report is divided into three main parts, the first being introductory. The second is devoted to the intercomparison of various theories, while in the final part the theories and the experiments are compared. Details of the lattice geometry and composition, and of the nuclear data used in the analysis, are given in the Appendices.

## 2. A description of the lattices

The lattice cell consists of a 90-rod fuel cluster, with a central stainless-steel tie rod, separated from the bulk moderator by an aluminium pressure tube, an air gap, and an aluminium calandria tube. The fuel rods lie with their centres on five concentric circles. Axially, the fuel rods have their ends inserted into aluminium end plates. This introduces a large perturbing effect, fuel and coolant being replaced by aluminium and air. A detailed description of this axial geometry is given in Reference [1]. These end plates are sufficiently far enough apart not to affect the fine structure and reaction rate measurements performed across the mid-plane. However, the perturbation effects on reactivity are quite sizeable.

Experiments were performed with five types of coolant in the clusters; the compositions of these coolants are listed in Table I.

TABLE I  
COOLANT COMPOSITIONS

Core	Coolant
5001 ...	Air
5002 ...	99.7% D <sub>2</sub> O, 0.3% H <sub>2</sub> O w/w
5003 ...	79.7% D <sub>2</sub> O, 20.3% H <sub>2</sub> O w/w
5004 ...	60.1% D <sub>2</sub> O, 39.9% H <sub>2</sub> O w/w
5005 ...	100% H <sub>2</sub> O

For simplicity these cores will be referred to in the text as containing air, 100% D<sub>2</sub>O, 80% D<sub>2</sub>O, 60% D<sub>2</sub>O and 100% H<sub>2</sub>O; the numbering corresponds to that of Reference [5]. However, all the calculations have been made with the exact compositions. The detailed dimensions of the lattices are given in the Appendix.

### 3. The measured bucklings: definition of the eigenvalue

The axial and radial bucklings given in Table II are taken from Table V of Reference [1]: the material buckling  $B_m^2$  is the algebraic sum of the radial and axial bucklings (all values are quoted in (metres)<sup>-2</sup>).

TABLE II  
AXIAL AND RADIAL BUCKLINGS

Core	$B_z^2$	$B_r^2$	$B_m^2$
5001	1.801 ± 0.026	-1.119 ± 0.104	0.682 ± 0.107
5002	1.913 ± 0.017	-0.953 ± 0.062	0.960 ± 0.064
5003	1.836 ± 0.011	-0.210 ± 0.037	1.626 ± 0.039
5004	1.924 ± 0.011	+0.002 ± 0.014	1.926 ± 0.018
5005	1.814 ± 0.013	-1.510 ± 0.020	0.304 ± 0.024

The material bucklings  $\tilde{B}_m^2$  quoted by Hyder et al. are defined by

$$\tilde{B}_m^2 = B_z^2 + \left(\frac{M_r}{M_z}\right)^2 \cdot B_r^2$$

$B_z^2$  and  $B_r^2$  are the measured values, while the migration area asymmetry  $(M_r/M_z)^2$  was calculated using an unpublished Mercury programme due to L. Pease and E. R. Cobb. These asymmetries are believed to be in error, and therefore no use has been made in this report of the material bucklings quoted by Hyder.

It is now conventional to test theoretical calculations of reactivity by computing  $k$ -effective for a geometric buckling equal to the measured material buckling, and this procedure has been followed in the present Report. This  $k_{eff}$ , which is often called the eigenvalue, should of course be equal to 1. Its departure from unity is a convenient measure of the accuracy of the theory.

## II. INTERCOMPARISON OF THEORETICAL METHODS

In this chapter, we find it convenient to use the measured material bucklings listed in Table II to compare theoretical predictions of  $k_{eff}$ . Comparison with measured reaction rates is deferred to Part III.

#### 4. Brief account of the methods of calculation

##### 4.1. The 5-group scheme

This scheme is described by ALLEN, HICKS and LESLIE [5]. It involves 3 fast and 2 overlapping thermal groups, covering the following energy ranges:

Group 1	10	MeV → 0.821 MeV
Group 2	0.821 MeV	→ 5.53 keV
Group 3	5.53 keV	→ 0.625 eV
Group 4 and 5	0.625 eV	→ 0

SANDPIPER computes the group-4 cross-sections on the assumption that the group-4 spectrum is identical with that which would be obtained in an infinite fuel region. Similarly the group-5 cross-sections are those obtained in a spectrum characteristic of an infinite moderator region; it therefore has a Maxwellian distribution.

It was soon realised, however, that there was an inconsistency in the assumptions: if the group-5 spectrum has a source in the moderator then the spectrum has an approximately  $1/E$  tail; but as the group-5 spectrum is a Maxwellian then it has no tail.

Furthermore, if we consider the energy dependence of the total flux, we see that the assumptions give a discontinuity at 0.625 eV: the group-3 flux is a little higher in the moderator than in the fuel. Also, when expressed in lethargy units, the group-3 flux does not show much variation over its lethargy range. Thus the flux at the bottom of group 3 will be almost constant across the lattice cell. On the other hand, the group-4 flux, which has a  $1/E$  tail, falls in the moderator, while the group-5 flux, which rises, has no tail. The top of the total thermal flux will therefore be distinctly higher in the fuel than in the moderator, and so cannot match the bottom of the group-3 flux.

It was therefore considered necessary to examine the effect of hardening the group-5 spectrum. As a first approximation the absorption in this group, which may be identified with the removal into it from group 3 was represented as an equivalent amount of  $1/v$  absorber in the moderator. This replaces the erstwhile Maxwellian spectrum in the moderator with a Wigner-Wilkins spectrum, and defines new group-5 cross-sections. As the values of the fluxes which determine the effective amount of  $1/v$  absorber are dependent on the cross-sections, the determination of the group-5 spectrum is an iterative process: in practice, one round of iteration is usually sufficient.

The then current version of SANDPIPER III always assumed that the group-5 spectrum was a Maxwellian at the temperature of the bulk moderator. The procedure adopted was to adjust this temperature so as to make

$$(\text{unit})_5 = \int_0^{0.625 \text{ eV}} \sqrt{\frac{E_0}{E}} \Phi_5(E) dE / \int_0^{0.625 \text{ eV}} \Phi_5(E) dE$$

the same as in the Wigner-Wilkins spectrum described in the previous paragraph. ("Unit" is the name given by AMSTER [4] to this ratio; the suffix 5 indicates that it is being calculated for the group-5 spectrum). This choice preserves the correct balance between leakage and  $1/v$  absorption. Minor errors are introduced owing to the  $U^{235}$  cross-section variation not being exactly  $1/v$ . Serious errors would be caused, however, if the temperature-hardened Maxwellians were used to obtain the effective cross-sections of the markedly non- $1/v$  absorbers ( $Pu^{239}$  and  $Lu^{176}$ ) when computing reaction-rate distributions. The effective group-5 cross-sections of all the detectors were therefore obtained from separate SOFOCATE calculations using  $1/v$  absorption-hardened spectra; these were then used with the fluxes from the temperature-hardened ARISTOS calculations. A similar correction should have been applied to the group-4 spectrum. This correction was found to be both small and difficult to apply; it was therefore ignored.

The effective temperatures for group 5 obtained from the final iterations are listed in Table III.

TABLE III

## FINAL TEMPERATURE ITERATION FOR GROUP-5 SPECTRUM

Core	Effective $T_5(^{\circ}K)$	$T_5(\text{eff})-293.3$
5001	450.5	157.2
5002	416.2	122.9
5003	396.6	103.3
5004	380.3	87.0
5005	372.0	78.7

As would be expected, the hardening of the group-5 spectrum diminishes as the amount of moderation in the channel increases. It must be emphasized that this spectrum-hardening is not available in SANDPIPER/ARISTOS as a normal option, and that it can only be inserted by a good deal of hand computation.

The SANDPIPER III library is based on the World 1960 Consistent Set and uses a value of 2.43 for  $\nu_{235}$ . A later recommended value is 2.438; the ARISTOS output has been modified accordingly. This correction is easy to make as ARISTOS outputs 2-group cross-sections; the thermal fission rate is modified and the reactivities re-computed. A more comprehensive discussion of cross-sections is given in Appendix 2.

In much of what follows, the word "ARISTOS" has been used as a mnemonic for the 5-group scheme.

#### 4.2. The 5-group Carlson calculations

Diffusion theory tends to underestimate fine structure effects. It is therefore necessary to check the validity of diffusion theory in the 5-group

scheme by comparison with a transport theory calculation. The cross-sections in this transport theory calculation are identical with those used in the (temperature-hardened) ARISTOS calculation. It follows that any discrepancies between the transport theory results and the corresponding ARISTOS results are due entirely to the difference between transport theory and diffusion theory.

The transport theory code used in these calculations was the Winfrith D.S.N. programme [17]. This is an IBM-7090 programme based on the discrete  $S_n$  method of B.G. CARLSON and G.I. BELL [19]. The decks of input data cards for this programme were prepared by the D.I.P. programme. This is a Mercury programme written by M.J. Roth which reads the SANDPIPER output tape, and punches out the cross-section data in the correct format.

#### 4.3. The 40-group Carlson calculations

These calculations, which are purely thermal, were made to check the validity of the two-thermal-group model which is used in the 5-group scheme. The Winfrith D.S.N. code was used with forty groups spanning the energy range  $0 \rightarrow 1\frac{1}{2}$  eV; the source flux above  $1\frac{1}{2}$  eV was assumed to be constant across the cell. The reaction rates for the energy range  $0 \rightarrow 0.625$  eV were then extracted from the results to provide parameters for comparison with the ARISTOS and 5-group Carlson results. The scheme is described in detail by M.J. TERRY [20]. The thermalization was represented by a free gas model with real atomic masses. The hyperfine-flux weighted element-number densities were obtained from the SANDPIPER output. The tie rod was treated as a region separate from the fuel. The fuel region extended from the outside of the tie rod to the inner edge of the pressure tube; the number densities were volume averaged over the whole of this region. These were used as data for the PXED programme [21], which outputs group cross-section data for the D.S.N. programme.

#### 4.4. Monte Carlo calculations of resonance absorption

SANDPIPER III calculates resonance integral of  $U^{238}$  from a correlation formula derived by Hicks from fundamental theory. The constants in this formula were obtained by fitting the Hellstrand measurements on single rods [8]. There are, however, uncertainties in the interpretation of these measurements and in their extension to rod clusters. In order to obtain a better estimate of the  $U^{238}$  resonance absorption, calculations have been performed by means of MOCUP, a Monte Carlo code for the IBM 7090 [9]. This code, with its present library, spans the energy range 4 eV to 10 keV and covers approximately 600 resonances. A little complication is introduced, when comparing with the SANDPIPER estimates, since this energy range is not the same as that spanned by group 3 of the 5-group scheme. It is simple to extract from the MOCUP results the fraction of those neutrons crossing the energy 5.53 keV which are absorbed by  $U^{238}$  before reaching 4 eV. The  $U^{238}$  resonance integral was then computed from the SANDPIPER formula over the energy range 5.53 keV to 4 eV, a correction being made to this formula for captures between 4 eV and 0.625 eV. This difference

between the MOCUP absorption and the modified SANDPIPER absorption was then added to the value of  $p$  calculated by the 5-group Carlson method to give the "best" value of resonance escape probability.

#### 4.5. The Benoist leakage model

The leakage model used in the ARISTOS programme is rather crude. The flux-weighted diffusion coefficient is averaged across the material regions of the lattice cell, the air gap being omitted from the calculation. The value so obtained is corrected by a simple volume factor to allow for the presence of the air gap. Because of the low cross-sections in aluminium, the pressure tube and calandria tube regions were treated as air gaps when calculating the cell-averaged diffusion coefficients. As a check, further calculations were performed in which the tubes were treated as matter rather than as air.

In order to obtain a better estimate of the leakage effects, calculations were made by the method proposed by Benoist [7]. The flux distributions required for this calculation were taken from the ARISTOS output, which is in a convenient form. It is considered that the use of Carlson fluxes rather than those given by ARISTOS would produce only small changes in the diffusion coefficients.

#### 5. Miscellaneous corrections

There are two further corrections to be made to both the ARISTOS and Carlson results. These are for the  $(n, 2n)$  reaction in the  $D_2O$ , and for the effect of the end plates.

##### 5.1. End-plate corrections

The fuel rods were held in position by aluminium end plates. As compared to a lattice of fuel rods which are infinite in the axial direction these endplates are equivalent to removing part of the fuel and coolant and replacing it by aluminium of reduced density. At the same time part of the steel tie rod is replaced by a bolt, which is similar to replacing part of the steel rod by steel of reduced density.

In order to correct the reactivity values for these end effects, and to obtain a theoretical determination of the axial flux distributions, a series of calculations were made with the two-dimensional diffusion theory code ANGIE (a 7090 FORTRAN programme) [22]. As it was not clear whether or not the coolant percolated into the gaps in the end plates, calculations were performed both with these gaps empty and with them full of coolant.

Some difficulty was experienced in running ANGIE, which was designed for problems very different from this. In particular, it repeatedly refused to accept the data for the 100%  $H_2O$  coolant core. Also the form of the output is not convenient for the present purpose: values of  $k_{inf}$  are given but a good deal of hand calculation is required to obtain the information required to calculate the leakage parameters. A simple scheme was therefore devised which could be written as a subroutine for subsequent programmes.

This scheme which uses little more than the information derived from the ARISTOS output, is based on the following three assumptions:

- (a) The effect of coolant entering the end-plate gaps is trivial and can be ignored. This assumption is valid as can be seen from the ANGIE results given in Table IV;
- (b) The effect of the axial flux variation can be ignored;
- (c) The radial flux distribution in the cell is independent of axial position and is the same at the ARISTOS-computed distributions with no end-plates.

TABLE IV  
END-PLATE EFFECTS ON  $k_{inf}$

Core	$\Delta k_{inf}$		
	ANGIE		CORAL
	Coolant in end-plates	No coolant in end-plates	No coolant in end-plates
5001	--	-0.92%	-1.14%
5002	-1.25%	-1.22%	-1.06%
5003	-1.90%	-1.93%	-1.70%
5004	-2.07%	-2.16%	-2.01%
5005	--	--	-2.22%

Assumptions (b) and (c) enable corrections to be made to the cell averaged cross-sections by first-volume weighting the cross-sections in the axial direction and then using the radial flux and volume-weighting factors derived from the ARISTOS output. The scheme has been used in CORAL, a Ferranti Mercury programme written by M. J. Roth. This programme accepts the ARISTOS output as input data together with further information such as the fraction of the total fuel-pack length which is end-plate, and the density reduction factors. It outputs new values of  $k_{inf}$ ,  $k_{eff}$  and cell-averaged cross-sections. Table IV shows a comparison of the effects of the end-plates on  $k_{inf}$  as calculated by ANGIE and by CORAL. It will be seen that the comparison between CORAL and ANGIE is good, thus justifying the approximations made in formulating the CORAL method.

The end-plates also affect the leakage. As well as calculating the change in  $k_{inf}$ , CORAL also gives a change in  $k_{eff}$  for an input value of buckling. For small changes of leakage this change in  $k_{eff}$  is linear with respect to the buckling and is given approximately by the following expression:

$$\Delta k_{eff} \approx \Delta k_{inf} - B^2 \cdot \Delta(L_t^2 + L_f^2)$$

TABLE V

## END-PLATE EFFECTS ON LEAKAGE

Core	Leakage component of reactivity change divided by the buckling
5001	+0.0042
5002	-0.0017
5003	-0.0015
5004	-0.0015
5005	-0.0015

where  $L_r^2$  and  $L_f^2$  are the thermal and fast migration areas. It follows that if the change in  $k_{eff}$  for unit buckling is computed, the change in  $k_{eff}$  for any other similar buckling can be found at once. Values of  $\Delta k_{eff} - \Delta k_{inf}$  for a buckling of one (metre)<sup>-2</sup> are given in Table V.

It will be seen that introducing the end-plates increases the leakage for all cores except for the air core. In the cores with liquid coolant, replacing the coolant by aluminium increases the leakage, since the scattering cross-section of aluminium is less than that of the coolant. In the air core there is no coolant to replace and so the aluminium decreases the leakage.

### 5.2. Correction for the (n, 2n) reaction

In both the ARISTOS and CARLSON calculations no allowance was made for the (n, 2n) reaction in D<sub>2</sub>O. In order to make the correction it was assumed that the introduction of the (n, 2n) cross-sections would not alter the flux shapes, and would therefore not alter the cell-averaged cross-sections for all other reactions. Thus, once the cell-averaged (n, 2n) cross-sections had been calculated using the existing fluxes, this together with the other (unaltered) cross-sections sufficed to re-compute the reactivities. The ARISTOS fluxes and cross-sections were used to calculate the (n, 2n) effect, it being assumed that the same corrections applied to the CARLSON results. Calculations were performed first by assuming that all the neutrons produced by the (n, 2n) reaction were born into group 1, and then the calculations were repeated with the assumption that all these neutrons were born into group 2. It will be seen from Table VI that the difference in reactivity between two extreme assumptions is negligible.

The (n, 2n) cross-section was computed from the list of energy dependent cross-sections given by CLARK [6]. When averaged over a typical group-1 spectrum a microscopic cross-section of 0.010 b was obtained.

### 6. The validity of diffusion theory

In the 5-group Carlson calculations the same macroscopic cross-sections were used as had been used in the temperature-hardened ARISTOS

TABLE VI

CORRECTIONS FOR (n, 2n) REACTION

Core	Increase in $k_{inf}$ due to (n, 2n) reaction	
	All (n, 2n) neutrons born into group 1	All (n, 2n) neutrons born into group 2
5001	0.47%	0.45%
5002	0.50%	0.49%
5003	0.44%	0.43%
5004	0.42%	0.41%
5005	0.31%	0.30%

calculations. Any discrepancies revealed by a comparison of the ARISTOS results with the 5-group Carlson results are therefore due entirely to the difference between diffusion theory and transport theory. Figures 1 to 5 show a comparison of the fluxes in each of the five groups in Core 5002 (100% D<sub>2</sub>O). The fluxes are normalized so that the mean flux in group 3 is equal to 1 in both calculations. It will be seen that there is good agreement in groups 2 and 3; there is fair agreement in group 4; but in groups 1 and 5, ARISTOS severely underestimates the flux variation. This is in line with the universal experience that diffusion theory underestimates flux vari-

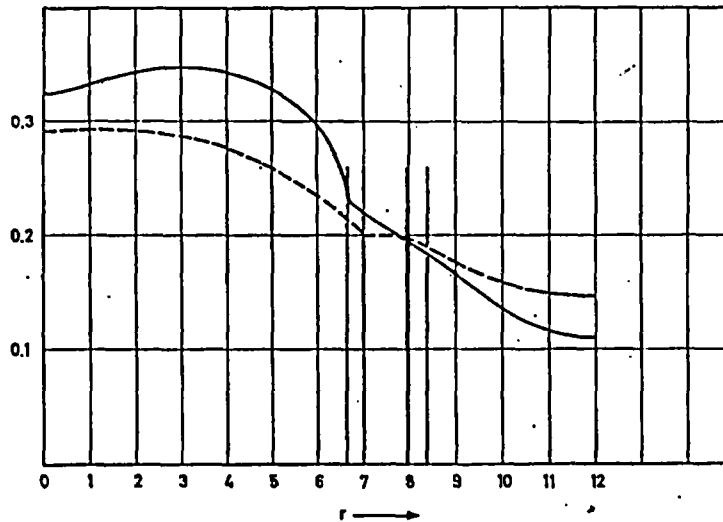


Fig. 1

Comparison of 5-group Carlson with ARISTOS. Core 5002: group-1 flux.

— Carlson  
 - - - ARISTOS

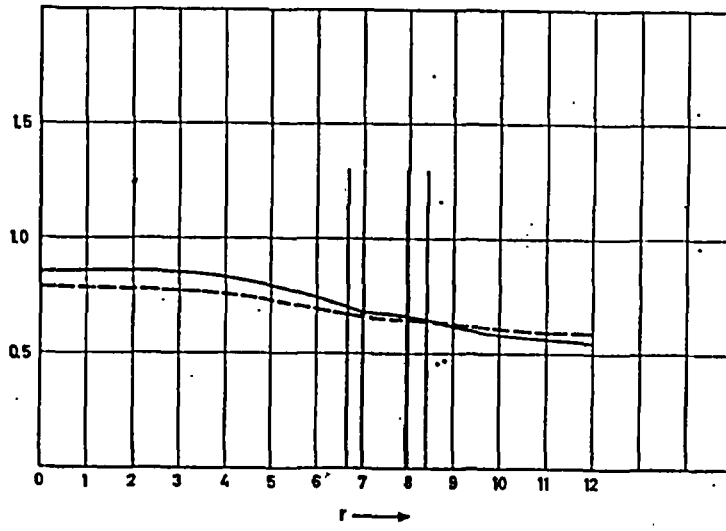


Fig. 2

Comparison of 5-group Carlson with ARISTOS. Core 5002: group-2 flux

— Carlson  
 - - - ARISTOS

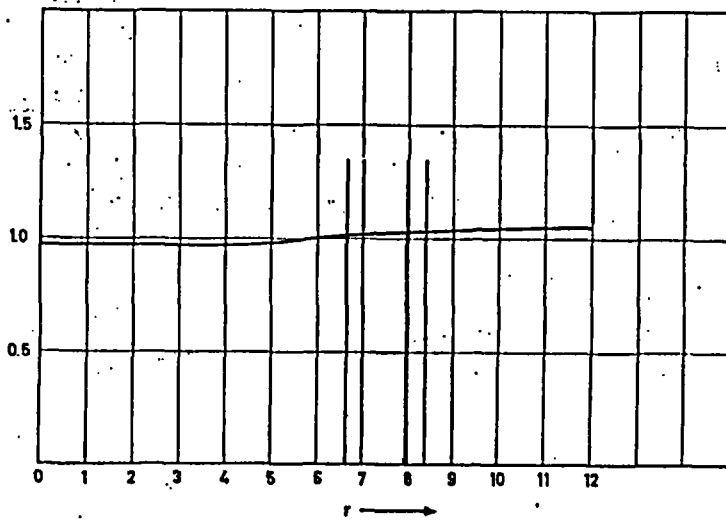


Fig. 3

Comparison of 5-group Carlson with ARISTOS. Core 5002: group-3 flux

— Carlson and ARISTOS

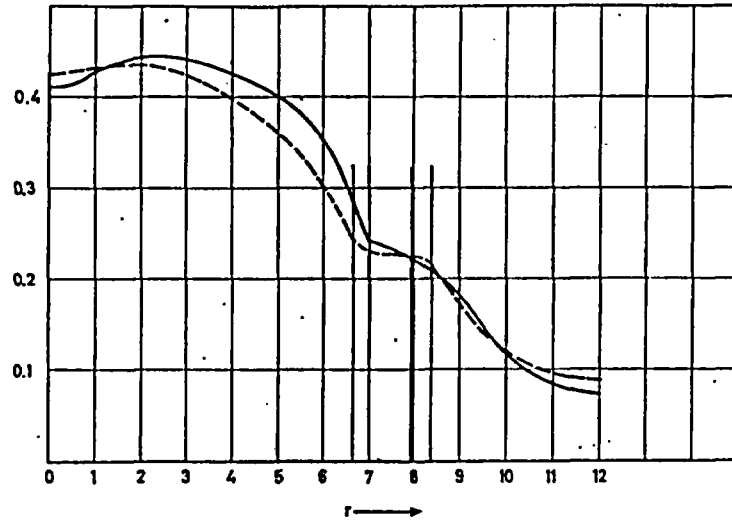


Fig. 4

Comparison of 5-group Carlson with ARISTOS. Core 5002: group-4 flux

— Carlson  
 - - - ARISTOS

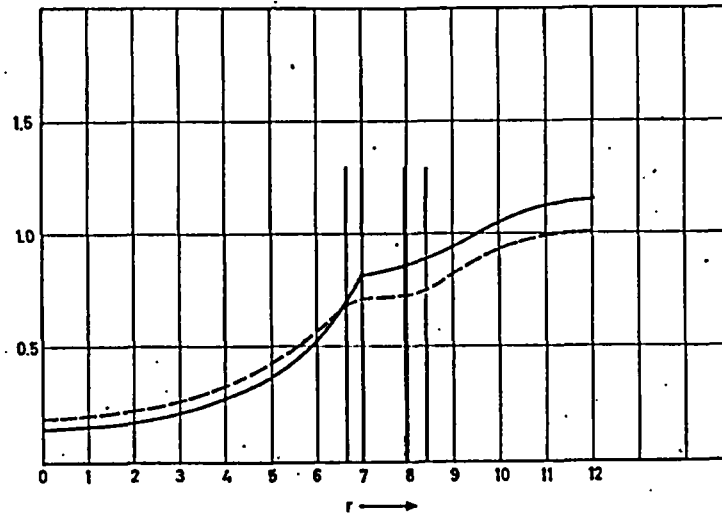


Fig. 5

Comparison of 5-group Carlson with ARISTOS. Core 5002: group-5 flux

— Carlson  
 - - - ARISTOS

ations. The fluxes for the other four cores showed the same general behaviour.

TABLE VII

## REACTIVITY BALANCE FOR CORE 5001

Parameter	5-group Carlson	ARISTOS	Reactivity difference
$(\eta)_t$	1.3420	1.3511	-0.60%
$\rho$	0.6560	0.6581	-0.18%
$(\eta)_f$	0.5013	0.4612	+1.38%
$k_{inf}$	1.0528	1.0468	+0.60%

TABLE VIII

## REACTIVITY BALANCE FOR CORE 5002

Parameter	5-group Carlson	ARISTOS	Reactivity difference
$(\eta)_t$	1.3212	1.3333	-0.82%
$\rho$	0.6748	0.6759	-0.10%
$(\eta)_f$	0.3988	0.3779	+0.68%
$k_{inf}$	1.0212	1.0236	-0.24%

TABLE IX

## REACTIVITY BALANCE FOR CORE 5003

Parameter	5-group Carlson	ARISTOS	Reactivity difference
$(\eta)_t$	1.2812	1.2933	-0.88%
$\rho$	0.7244	0.7269	-0.22%
$(\eta)_f$	0.3990	0.3763	+0.62%
$k_{inf}$	1.0381	1.0429	-0.48%

## 6.1. General reactivity balance

It is to be expected that the different flux shapes computed according to the two methods will result in different reactivities. Tables VII to XI show the reactivity balance for the five cores. For the purpose of com-

TABLE X  
REACTIVITY BALANCE FOR CORE 5004

Parameter	5-group Carlson	ARISTOS	Reactivity difference
$(\eta f)_t$	1.2458	1.2575	-0.89%
p	0.7583	0.7612	-0.24%
$(\eta f)_f$	0.4055	0.3785	+0.64%
$k_{inf}$	1.0427	1.0476	-0.49%

TABLE XI  
REACTIVITY BALANCE FOR CORE 5005

Parameter	5-group Carlson	ARISTOS	Reactivity difference
$(\eta f)_t$	1.1513	1.1622	-0.89%
p	0.8170	0.8196	-0.19%
$(\eta f)_f$	0.4285	0.3949	+0.60%
$k_{inf}$	1.0190	1.0238	-0.48%

parison the 5-groups have been condensed to 2-groups in the way described by LESLIE et al. [3]. The 2-group equation for  $k_{inf}$  is then

$$k_{inf} = (\eta f)_t p + (\eta f)_f (1 - p)$$

The quantities in this equation are related to the cell-averaged cross-sections defined by Leslie et al. by

$$(\eta f)_t = (\nu \Sigma_f)_t / \Sigma_{at}$$

$$(\eta f)_f = (\nu \Sigma_f)_f / \Sigma_{af}$$

$$p = \Sigma_{ff} / (\Sigma_{af} + \Sigma_{ff})$$

It should be noted that  $(\nu \Sigma_f)_t$  includes epithermal fissions in  $U^{235}$  as well as fast fissions in  $U^{238}$ . (The suffices t and f refer to the thermal and fast groups respectively).

The reactivity differences due to the discrepancies between the components are then given by

$$\partial k / \partial (\eta f)_t = p,$$

$$\partial k / \partial p = (\eta f)_t - (\eta f)_f,$$

$$\partial k / \partial (\eta f)_f = 1 - p$$

It will be seen from Tables VII to XI, that there is a pattern in the discrepancies. In all cores diffusion theory overestimates the thermal contribution to reactivity and underestimates the fast contribution. This is to be expected from the fine structure distributions. By underestimating the thermal fine structure, diffusion theory underestimates the absorption in the pressure tube and calandria tube. By underestimating the group-1 fine structure, diffusion theory underestimates the fast-fission factor. It follows that the discrepancies between transport and diffusion theory are greater than are suggested by the differences in  $k_{inf}$ ; the relatively small discrepancies in total reactivity are due to the partial cancellation of the large fast and thermal contributions.

## 6.2. The thermal region

Table XII shows the fractions of the thermal neutrons absorbed in each region of core 5002. It shows that there is a marked discrepancy between the two estimates of group-5 absorption in the calandria tube. The results for the other four cores are similar.

TABLE XII

### THERMAL ABSORPTION IN CORE 5002

Region	Fraction of thermal absorptions which occur in group 4		Fraction of thermal absorptions which occur in group 5	
	Carlson	ARISTOS	Carlson	ARISTOS
Tie rod	0.01192	0.01244	0.00636	0.00811
Fuel	0.36311	0.33359	0.53785	0.57510
Pressure tube	0.00473	0.00444	0.02206	0.01939
Calandria	0.00731	0.00742	0.04340	0.03658
Moderator	0.00020	0.00025	0.00306	0.00268

The reactivity differences due to these various thermal fine structure effects can be obtained as follows:-

$$(\eta f)_t = \eta(\text{fuel}) \cdot f(\text{fuel})$$

$$= \eta(\text{fuel}) \cdot \{1 - q(\text{tie rod}) - q(\text{press. tube}) - q(\text{cal. tube}) - q(\text{mod.})\}$$

where the  $q$  terms denote the fractions of thermal neutrons absorbed in the various regions. It thus follows that the reactivity differences are given by

$$\Delta k_{\text{inf}} = p \Delta(\eta f)_t$$

$$= p f(\text{fuel}) \cdot \Delta \eta(\text{fuel})$$

$$- p \eta(\text{fuel}) \cdot \{\Delta q(\text{tie rod}) + \Delta q(\text{press. tube}) + \Delta q(\text{cal. tube}) + \Delta q(\text{mod.})\}.$$

These reactivity components are listed in Table XIII

TABLE XIII

DIFFERENCE BETWEEN 5-GROUP CARLSON AND ARISTOS  
CALCULATIONS OF THERMAL CONTRIBUTIONS TO REACTIVITY

CORE					
Component	5001	5002	5003	5004	5005
$\eta(\text{fuel})$	0	-0.05%	-0.02%	-0.02%	-0.01%
Tie rod	+0.24%	+0.22%	+0.20%	+0.18%	+0.09%
Pressure tube	-0.23%	-0.29%	-0.32%	-0.33%	-0.32%
Calandria	-0.57%	-0.66%	-0.70%	-0.69%	-0.62%
Moderator	-0.04%	-0.04%	-0.04%	-0.03%	-0.03%
Total	-0.60%	-0.82%	-0.88%	-0.89%	-0.89%

### 6.3. The fast region

It will be seen from Fig. 3 that the group-3 fluxes are almost identical when calculated by ARISTOS and by the 5-group Carlson method. It follows that the differences in the values of  $(\eta f)_f$  must be due to the fission and absorption processes in groups 1 and 2. The discrepancy is therefore mainly due to the fast-fission factor.

In the Harwell experiments, the ratios of  $U^{238}$  fissions to  $U^{235}$  fissions were measured for each ring of fuel elements. For comparison these ratios were also calculated by means of ARISTOS and from the Carlson results. The expression for this reaction ratio,  $\delta_{28}$ , is:

$$\delta_{28} = \frac{N_{28} \cdot \sigma_{f1}^{28} \cdot \bar{\Phi}_1}{N_{25} \left\{ \sigma_{f1}^{25} \bar{\Phi}_1 + \sigma_{f2}^{25} \bar{\Phi}_2 + \sigma_{f3}^{25} \bar{\Phi}_3 \right\} + N_{25}^1 \sigma_{ft} \bar{\Phi}_t}$$

where  $N_{28}$  and  $N_{25}$  are the element number densities in the fuel rod, while  $N_{25}^1$  is the number density multiplied by the (thermal) hyperfine flux weighting factor for the fuel rod. The fluxes  $\bar{\Phi}_i$  are the region averaged fluxes. In the ARISTOS calculations  $\sigma_{ft} \bar{\Phi}_t$  represents  $\sigma_{f4} \bar{\Phi}_4 + \sigma_{f5} \bar{\Phi}_5$ . In the CARLSON calculations,  $\bar{\Phi}_1 \bar{\Phi}_2 \bar{\Phi}_3$  are the fluxes obtained from the 5-group Carlson results, while  $\sigma_{ft} \bar{\Phi}_t$  is obtained from the normalized forty-group Carlson calculations discussed in section 7.

There is a simple relation between the fission ratio and  $k_{inf}$ . The expression governing the fluxes in the fast groups is

$$(\Sigma_{ai} + \Sigma_{fi}) \Phi_i = \chi_i \cdot S \cdot \frac{(1+\Delta)}{k_{inf}} + \Sigma_{r1-1} \Phi_{i-1}$$

where  $S$  represents the fission source without  $U^{238}$  fissions, that is

$$S = \text{Sum}_i N_{25} \cdot (\nu \sigma_f)_i^{25} \Phi_i,$$

while

$$\Delta = \text{Sum}_i N_{28} \cdot (\nu \sigma_f)_i^{28} \Phi_i / \text{Sum}_i N_{25} \cdot (\nu \sigma_f)_i^{25} \Phi_i.$$

The notation conforms to that of LESLIE *et al.* [3]. It will be seen that  $1+\Delta$  is the proportional increase in reactivity due to the  $U^{238}$  fissions. As most of the  $U^{235}$  fissions are thermal, this may be written

$$\Delta \approx \delta_{28} (\nu_{28}^1 / \nu_{25}^{th})$$

Therefore  $1 + \delta_{28} (\nu_{28}^1 / \nu_{25}^{th})$  is very nearly the contribution of  $U^{238}$  fission to reactivity. We thus define

$$\Delta k(U_{238} \text{ fission}; \text{CARLSON-ARISTOS}) = \frac{\left\{ 1 + \delta_{28} (\nu_{28}^1 / \nu_{25}^{th}) \right\}_{\text{CARLSON}}}{\left\{ 1 + \delta_{28} (\nu_{28}^1 / \nu_{25}^{th}) \right\}_{\text{ARISTOS}}} - 1$$

Table XIV shows a comparison of these quantities with the fast reactivity discrepancies extracted from Tables VII to XI. This Table confirms that these discrepancies are mostly due to  $U^{238}$  fission.

TABLE XIV

FAST-FISSION REACTIVITY DISCREPANCIES

Core	$\Delta k$ ( $U^{235}$ fiss; Carlson-ARISTOS)	$(1-p) \Delta(\eta)_f$
5001	1.52%	1.38%
5002	0.63%	0.68%
5003	0.59%	0.62%
5004	0.61%	0.64%
5005	0.64%	0.60%

As the cylindrical cell approximation can introduce serious errors into transport theory calculations, it was necessary to check that the Carlson calculations were not being affected in this way. This was done by comparing the results of a one-group Carlson calculation in a cylindrical cell with a Monte Carlo calculation in an equivalent square cell. The Monte Carlo calculation was performed by K. Howie of the English Electric Company, Ltd., using the same macroscopic cross-sections as were used in the Carlson calculation. In the calculations the pressure tube, gas channel and calandria tube were smeared into a single region to produce a three-region assembly; the source distribution was obtained from ARISTOS. The aim was to produce a system which was simple but at the same time sufficiently similar to the 5004-core lattice cell to test the effect of the cylindrical cell approximation on the group-1 flux. The normalized region-averaged fluxes are given in Table XV.

TABLE XV

COMPARISON OF FLUX IN A CYLINDRICAL CELL WITH THAT IN A SQUARE CELL

Region	Flux in cylindrical cell by Carlson method	Flux in square cell by Monte Carlo
Fuel	2.648	2.630
Tubes + gas gap	1.575	1.580
Moderator	1	1

The uncertainty in the Monte Carlo results was estimated to be of the order of 1%. It is thus seen that the error introduced into the Carlson calculation by the cylindrical cell approximation is negligible.

## 7. The validity of the two-thermal-group model

In the last section the validity of diffusion theory was examined by comparing ARISTOS calculations with the 5-group Carlson results. In this section, discussion is confined to the thermal region. The validity of the two-thermal-group spectrum model will be investigated by comparing the 5-group Carlson results with the results obtained from the 40-group Carlson calculations. In this way a comparison is obtained between the spectrum models without introducing the errors inherent in diffusion theory. Table XVI shows a comparison of the values of  $(\eta^f)_t$ , together with the reactivity differences caused by the discrepancies.

TABLE XVI

REACTIVITY ERRORS DUE TO TWO-THERMAL-GROUP SPECTRUM MODEL (40-GROUP CARLSON MINUS 5-GROUP CARLSON)

Core	$(\eta^f)_t$ 40-group Carlson	$(\eta^f)_t$ 5-group Carlson	$\Delta k$
5001	1.3294	1.3420	-0.82%
5002	1.3222	1.3212	+0.07%
5003	1.2925	1.2812	+0.82%
5004	1.2572	1.2458	+0.86%
5005	1.1582	1.1513	+0.57%

A comparison of the thermal absorptions in each region is given in Tables XVII and XVIII for cores 5001 and 5002. The values for core 5002 are typical of those for all the liquid-filled cores. In all except the air core the thermal-flux distribution is flatter when calculated by the 40-group Carlson method.

TABLE XVII

## THERMAL ABSORPTIONS IN CORE 5001

	40-group Carlson	5-group Carlson	$\Delta q$
Tie rod	0.02145	0.02057	-0.00088
Fuel	0.90735	0.90832	-0.00097
Pressure tube	0.02329	0.02335	+0.00006
Calandria tube	0.04479	0.04473	+0.00006
Moderator	0.00312	0.00303	+0.00009

TABLE XVIII

## THERMAL ABSORPTIONS IN CORE 5002

	40-group Carlson	5-group Carlson	$\Delta q$
Tie rod	0.01940	0.01828	+0.00112
Fuel	0.90680	0.90096	+0.00584
Pressure tube	0.02450	0.02679	-0.00229
Calandria tube	0.04626	0.05071	-0.00445
Moderator	0.00304	0.00326	-0.00022

The reactivity discrepancies due to differences in  $\eta$  and in the fractional absorption in each region are listed below in Table XIX.

It will be seen that in the liquid-filled cores there are two opposing contributions to the reactivity differences. The 40-group Carlson calculations give a lower value of  $\eta(\text{fuel})$ , which is more than cancelled by the reduced fine structure and the consequent smaller absorption outside the coolant channel. In the air core, the 40-group Carlson also gives the higher fine structure.

TABLE XIX

REACTIVITY DIFFERENCE COMPONENTS BETWEEN  
40- AND 5-GROUP CARLSONS

Component	5001	5002	5003	5004	5005
$\eta(\text{fuel})$	-0.73%	-0.51%	+0.02%	-0.01%	-0.37%
Tie rod	-0.08%	-0.11%	-0.12%	-0.12%	-0.13%
Pressure tube	+0.01%	+0.23%	+0.30%	+0.33%	+0.36%
Calandria tube	-0.01%	+0.44%	+0.60%	+0.64%	+0.68%
Moderator	-0.01%	+0.02%	+0.02%	+0.02%	+0.03%
Total	-0.82%	+0.07%	+0.82%	+0.86%	+0.57%

## 8. The validity of the SANDPIPER resonance integral,

The resonance absorptions were calculated by means of the MOCUP programme. These were then used to obtain correction factors for the 5-group Carlson values of  $p$  as described in section 4.4. The effects of these corrections are large as can be seen from Table XX.

It will be seen that the corrections to the 5-group Carlson values are negative except for the  $D_2O$  core. The statistical uncertainties in the MOCUP

TABLE XX

## MONTE CARLO CORRECTIONS TO RESONANCE ESCAPE PROBABILITY

Core	p (5-group Carlson)	$\Delta p$ (MOCUP)	p (corrected)	$\Delta k$
5001	0.6560	$-0.0150 \pm 0.003$	0.6410	-1.26%
5002	0.6748	$+0.0090 \pm 0.003$	0.6838	+0.83%
5003	0.7244	$-0.0093 \pm 0.003$	0.7151	-0.82%
5004	0.7583	$-0.0067 \pm 0.003$	0.7516	-0.56%
5005	0.8170	$-0.0064 \pm 0.003$	0.8106	-0.46%

calculations amount to approximately 0.3% in reactivity. BRIGGS [18] has shown by an extended series of calculations that the apparently anomalous result for the  $D_2O$  is genuine, and is not due either to error or to statistical uncertainty.

## 9. Comparison of the ARISTOS and Benoist leakage models

The leakage parameters were computed by the Benoist model, using the ARISTOS fluxes, as described in section 4.5. The value of slowing down and thermal diffusion areas (in  $cm^2$ ) are given in Table XXI.

## 10. Summary of theoretical reactivities

The so-called "best" method of calculation consists of computing  $(\eta f)_t$  by the 40-group Carlson method,  $(\eta f)_t$  by the 5-group Carlson method,

TABLE XXI

## COMPARISON OF VARIOUS LEAKAGE MODELS

Core	Benoist model				ARISTOS model			
	Tubes treated as void				Tubes treated as void		Tubes treated as matter	
	$L_{tz}^2$	$L_{tr}^2$	$L_{tz}^2$	$L_{tr}^2$	$L_t^2$	$L_f^2$	$L_t^2$	$L_f^2$
5001	110.18	100.19	332.16	305.31	94.99	320.04	103.11	302.71
5002	99.95	89.14	208.86	192.54	80.82	182.26	95.44	182.98
5003	88.84	77.65	165.47	152.12	68.78	139.87	85.50	142.01
5004	78.74	67.98	143.34	131.94	61.71	125.00	77.54	125.38
5005	67.63	64.99	108.74	100.03	49.49	95.12	64.15	95.31

$p$  by the 5-group Carlson method together with the MOCUP corrections,  $L_t^2$  and  $L_f^2$  by the Benoist method.

$k_{eff}$  is obtained, for any particular method of calculation, by substituting into the following equations:

$$k_{eff} = \frac{(\eta f)_t p}{(1+B^2 L_t^2)(1+B^2 L_f^2)} + \frac{(1-p)(\eta f)_f}{(1+B^2 L_f^2)} + \Delta k(n, 2n) + \Delta k(\text{end effects})$$

where

$$B^2 L_t^2 = B_z^2 L_{tz}^2 + B_r^2 L_{tr}^2,$$

$$B^2 L_f^2 = B_z^2 L_{fz}^2 + B_r^2 L_{fr}^2.$$

The last two terms represent the corrections described in sections 5.1 and 5.2. If theory and experiment were in perfect agreement then inserting the measured material bucklings into these equations would make  $k_{eff}$  equal to unity. Thus the difference between  $k_{eff}$  and unity gives the reactivity discrepancy for the particular method of calculation. This number, which is called "the eigenvalue" is the standard criterion of the excellence (or otherwise) of the method.

We shall be presenting the eigenvalues given by the various methods later in this section. However it is convenient to begin by presenting the various values of  $k_{inf}$ . This shows the reactivity discrepancies due to changes in theory without any (possibly confusing) reference to the experimental results. The difference between  $k_{inf}$  (ARISTOS corr.) and  $k_{inf}$  (Best) shows the error which would be introduced by using ARISTOS computed parameters throughout in the criticality equation

$$k_{inf} = (\eta f)_t p + (\eta f)_f (1-p) + \Delta k(n, 2n) + \Delta k(\text{end-effects}).$$

The results are presented in Table XXII, from which it will be seen that the differences are fairly small,  $\sim 1.0\%$ . This is due, however, to partially cancelling errors. (The first line of this Table gives the sum of the first two terms in this criticality equation. The second line gives the change in the first term due to temperature hardening of the group-5 spectrum, while the third and fourth lines give the magnitude of the fourth and third terms of the equation). The values listed as  $k_{inf}$  (ARISTOS corrected) may be regarded as the true predictions of the 5-group scheme for this experiment. The temperature-hardening of the group-5 spectrum is wholly compatible with this scheme, and is included in the METHUSELAH programme (see section 10.2 below). Also an adequate description of the experiment must obviously include the  $(n, 2n)$  reaction and the effect of the

TABLE XXII  
CORRECTIONS TO THE ARISTOS VALUES OF  $k_{inf}$

Core	5001	5002	5003	5004	5005
$k_{inf}$ (ARISTOS)	1.0551	1.0282	1.0408	1.0454	1.0203
Temp. hardening	-0.83%	-0.46%	+0.21%	+0.22%	+0.35%
End effects	-1.14%	-1.06%	-1.70%	-2.01%	-2.22%
(n, 2n)	+0.45%	+0.49%	+0.43%	+0.41%	+0.30%
$k_{inf}$ (ARISTOS corr.)	1.0399	1.0179	1.0302	1.0316	1.0046
5-group Carlson	+0.60%	-0.24%	-0.48%	-0.49%	-0.48%
40-group Carlson	-0.82%	+0.07%	+0.82%	+0.86%	+0.57%
MOCUP	-1.26%	+0.83%	-0.83%	-0.56%	-0.46%
	$\pm 0.03\%$				
$k_{inf}$ (Best)	1.0251	1.0245	1.0253	1.0297	1.0009
	$\pm 0.0003$				

end-fittings. On the other hand, corrections below this line may be regarded as revealing short-comings which are inherent in the 5-group scheme. Similar remarks apply to the entries in Table XXIII.

A similar Table can be constructed for the effects on  $k_{eff}$ . These are complicated by the effect of the end-fittings in changing the leakage. In the air core the end-effects reduce the leakage. In the other cores, the aluminium, by replacing coolant, increases the leakage. This is shown in section 5.1; Table V. The other corrections are nearly equal to the corresponding corrections on  $k_{inf}$ . For instance, the correction to  $k_{inf}$  for replacing the two thermal groups by the 40-group Carlson values is given by:

$$\Delta k_{inf} = p \cdot \Delta(\eta f)_t$$

whereas the correction to  $k_{eff}$  is given by

$$\Delta k_{eff} = \frac{p \cdot \Delta(\eta f)_t}{(1+B^2 L_t^2)(1+B^2 L_f^2)}$$

Since the leakage is small in all these cores, these corrections are nearly equal. Table XXIII shows the corrections to  $k_{eff}$ . It will be seen that the eigenvalues given by the "best" method are low in all cores.

TABLE XXIII  
CORRECTIONS TO THE ARISTOS VALUES OF  $k_{eff}$

Core	5001	5002	5003	5004	5005
$k_{eff}$ (ARISTOS)	1.0281 ±0.0047	1.0044 ±0.0020	1.0076 ±0.0010	1.0101 ±0.0004	1.0158 ±0.0004
Temp. hardening.	-0.92%	-0.52%	+0.19%	+0.19%	0.36%
End effects	-0.85%	-1.22%	-1.94%	-2.30%	-2.27%
(n, 2n)	+0.45%	+0.49%	+0.43%	+0.41%	+0.30%
$k_{eff}$ (ARISTOS, corr.)	1.0149 ±0.0047	0.9919 ±0.0020	0.9944 ±0.0010	0.9931 ±0.0004	0.9997 ±0.0004
Benoist leakage	-0.53%	-0.65%	-0.75%	-0.65%	-0.26%
5-group Carlson	+0.59%	-0.23%	-0.45%	-0.46%	-0.47%
40-group Carlson	-0.80%	+0.07%	+0.79%	+0.83%	+0.56%
MOCUP	-1.19% ±0.03%	+0.80% ±0.03%	-0.79% ±0.03%	-0.54% ±0.03%	-0.46% ±0.03%
$k_{eff}$ (Best)	0.9956 ±0.0050	0.9917 ±0.0023	0.9824 ±0.0013	0.9849 ±0.0007	0.9934 ±0.0007

10.1. The derivation of  $k_{inf}$  from the experimental bucklings

Defining "F" and "T" by

$$F = 1 + B_z^2 L_{z2}^2 + B_r^2 L_{fr}^2,$$

$$T = 1 + B_z^2 L_{tz}^2 + B_r^2 L_{tr}^2,$$

we have for a just critical assembly

$$1 = \frac{(\eta f)_t p}{F T} + \frac{(1-p)(\eta f)_f}{F} + \Delta k_{eff} (\text{end-effects}) + \Delta k (n, 2n).$$

The equation for  $k_{inf}$  is.

$$k_{inf} = (\eta f)_t p + (1 - p) (\eta f)_f + \Delta k_{inf} (\text{end-effects}) + \Delta k (n, 2n).$$

It follows from these equations that

$$k_{inf} = FT - X$$

where

$$X = (1 - p) (\eta f)_f (T - 1) + FT \cdot \Delta k_{eff} (\text{end-effects})$$

$$- \Delta k_{inf} (\text{end-effects}) + (FT - 1) \cdot \Delta k (n, 2n).$$

The "experimental"  $k_{inf}$  is obtained by calculating all the parameters except the bucklings, and then inserting the experimental bucklings into this equation. The term "X" is a small leakage-dependent correction. Apart from this term, the  $k_{inf}$  is being inferred from the experimental bucklings on the assumption that the theoretical leakage parameters are correct. A comparison of the theoretical and experimental values of  $k_{inf}$  are given in Table XXIV.

TABLE XXIV

COMPARISON OF EXPERIMENTAL AND THEORETICAL  $k_{inf}$

Core	$k_{inf}$ (theory)	$k_{inf}$ (expt.)	X
5001	1.0251 ± 0.0003	1.0302 ± 0.0050	0.0043
5002	1.0245 ± 0.0003	1.0329 ± 0.0023	-0.0005
5003	1.0253 ± 0.0003	1.0435 ± 0.0013	-0.0014
5004	1.0297 ± 0.0003	1.0454 ± 0.0007	-0.0022
5005	1.0009 ± 0.0003	1.0075 ± 0.0007	-0.0004

It will be seen that the discrepancies between the theoretical and experimental values of  $k_{inf}$  are almost the same as the discrepancies between the values of  $k_{eff}$  and unity listed in Table XXIII. Before drawing conclusions, however, it must be remembered that the theoretical values of slowing-down and thermal diffusion areas were used in deriving the experimental values of  $k_{inf}$ .

## 10.2. A later version of the Winfrith 5-group scheme

After much of the work in this report had been done an IBM-7090 programme METHUSELAH, which combines the functions of SANDPIPER III and ARISTOS, was completed (16). This programme contains certain improvements in the theory. It also allows burnup calculations to be made, though this is not important in the present application. A comparison of METHUSELAH and ARISTOS results is given in Table XXV. Both sets of results are corrected for end-effects, (n, 2n) effects, and temperature hardening.

TABLE XXV

## COMPARISON OF METHUSELAH WITH ARISTOS

Core	5001	5002	5003	5004	5005
$k_{eff}$ (ARISTOS)	1.0149	0.9919	0.9944	0.9931	0.9997
$k_{eff}$ (METHUSELAH)	1.0174	0.9937	0.9944	0.9905	0.9985

It will be seen that the differences between the ARISTOS and METHUSELAH results are small but not insignificant. (The number quoted corresponds to the fifth line of Table XXIII).

## III. COMPARISON OF EXPERIMENT WITH THEORY

In this chapter the measured reaction rates are compared with the theoretical predictions. The effects upon reactivity of the discrepancies between theory and experiment are also discussed.

## 11. Manganese activation fine structure

In Table VI of their report, HYDER et al. give the manganese reaction rates at various positions across the lattice cell. Figure 15 of the same report gives a plot of these values. In the fuel bundle, the centre foil was positioned in the tie rod while the remaining foils were placed on the outside of the cans on the side facing the calandria tube. The measurements in the moderator were made at various positions along the cell boundary. The values were normalized to unity at position  $d_3$  (the foil on the third fuel ring).

## 11.1. Modification of the experimental values

The theoretical values which are to be compared with experiment have been computed for a cylindrical cell. It is necessary to reduce the values measured in the moderator to a similar basis so that a proper comparison

can be made. A method is given by E. R. COHEN [10] for predicting the flux in a square lattice cell by diffusion theory. In particular, an expression for the flux along the cell boundary is given from which can be found a boundary position for which the flux is the same as the flux on the boundary of the equivalent cylindrical cell. This occurs when  $z/a = 0.2970$  where "a" is the cell width and "z" is the distance from the corner of the cell. In order that a comparison might be made with experiment, the Cohen formula was fitted to the experimental reaction rates at the cell corner and the mid-point of the cell boundary. The value of the reaction rate at the equivalent cylindrical cell position was then read off the Cohen curve. This interpolated value was then plotted on the main graph at a radius equal to that of the equivalent cylindrical cell. The process is demonstrated in Fig. 6. The other two experimental values on the boundary are also plotted. It will be seen that they lie very close to the Cohen curve; this was also true for the other cores.

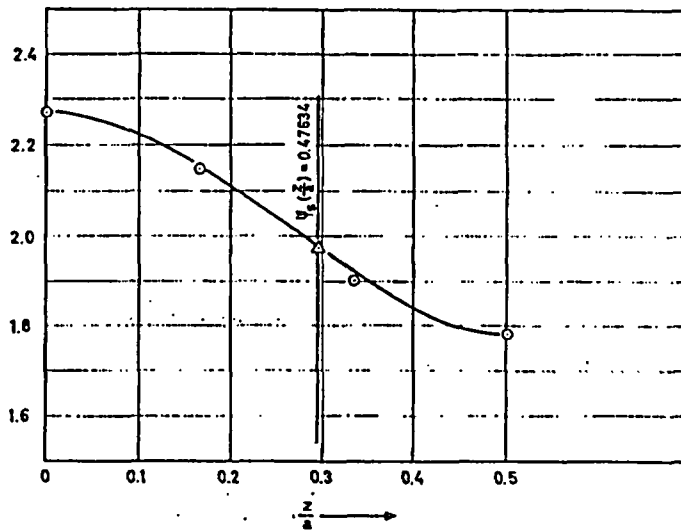


Fig. 6

Method of interpolating the boundary values of manganese fine structure to give the equivalent cylindrical cell boundary value. Core 5002.

- Theoretical curve
- Experimental values
- △ Interpolated value

The calculated values in the fuel bundle should be corrected by a hyperfine flux weighting factor. The hyperfine factors calculated by SANDPIPER are mean values for the fuel, sheath, and coolant; all the detector foils, with the exception of the centre one, lie on the boundaries of the clad and coolant. It is, therefore, not clear what the correct hyperfine flux-weighting factor should be. It is reasonable to suppose, however, that the hyperfine factor for the foils should be just a little higher than the value for the clad. As the mean value for the clad is a little less than unity, it was decided to ignore the hyperfine weighting for the off-centre foils. The

effects of hyperfine weighting are in any case small as can be seen from the values for core 5005 which has the most pronounced hyperfine structure:

$$W_f = 0.95, \quad W_{\text{clad}} = 0.98, \quad W_{\text{coolant}} = 1.04.$$

However, the central foil lies within the tie rod so that a hyperfine correction is needed for it. In order not to have a discontinuous theoretical curve, the experimental values for this position were divided by the theoretical hyperfine weighting factor for the tie-rod. Thus the experimental values on the cell boundary and the centre value have been modified in the way described above to permit a direct comparison with the theory. All the other experimental values are unchanged. On the Figures, these modified values are distinguished from values derived directly from the experiments.

### 11.2. Manganese self-shielding

HYDER et al. [14] have argued that there is a considerable resonance self-shielding effect in the detector foils. The report quotes an experimental value of 1.00 for the ratio of episcadmium resonance integral to the 2200 m/s cross-section: the value deduced from basic nuclear data is 1.38. This implies that self-shielding reduces the resonance integral in the foils by a factor  $1/1.38 = 0.72$ .

The shielded value of the resonance integral has been used when calculating the manganese reaction rate. That is, the value measured experimentally for the actual foils is used; the question of whether there really is a self-shielding effect, or whether the theoretical resonance integral is incorrect, is thus avoided. The effect of this self-shielding factor of  $1/1.38$  on the distribution of the bare manganese reaction rate is small for all cores. Figure 7 shows the effect for core 5001.

### 11.3. Discussion of the comparison of theory with experiment

The manganese reaction-rate distributions were first computed by the SANDPIPER and ARISTOS programmes. For all cores except 5005, the theoretical values were normalized to the experimental value at the outside face of the pressure tube. In the case of core 5005, the experimental rise across the pressure tube is suspiciously large; the theoretical curve was therefore normalized to the experimental value at the inside face of the pressure tube. It will be seen that the distributions given by SANDPIPER/ARISTOS are too flat in all cases (see Figs. 8 to 12); in particular, the flux rise in the moderator is underestimated.

In order to check the effect of using diffusion theory, the 5-group Carlson calculations (see section 4.2) were compared with experiment for cores 5001, 5002 and 5005. It will be seen from Figs. 8, 9 and 12 that these Carlson values give a more pronounced fine structure than do the ARISTOS values. The defects of diffusion theory are considerably over-corrected, and the agreement with experiment is poor.

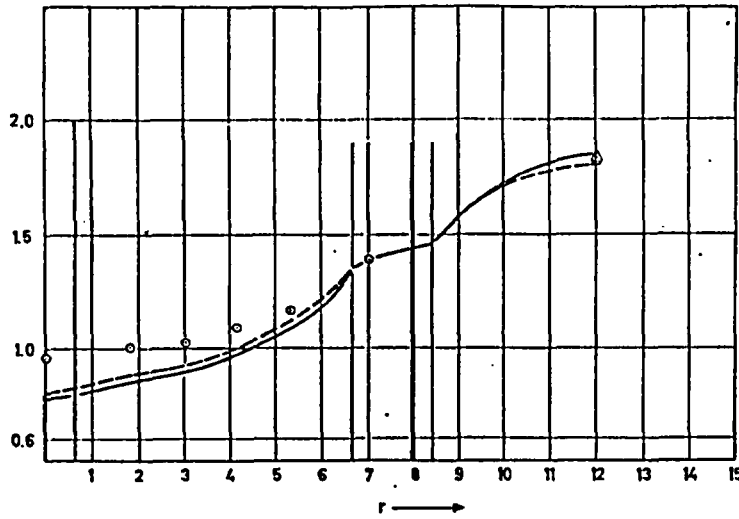


Fig. 7

Manganese reaction rate. Comparison of theory with experiment core 5001; air core 3-plus-40 group Carlson values. The effect-of resonance shielding.

- Corrected for resonance shielding
- No resonance shielding
- Unmodified experimental values
- △ Modified experimental values  
(See section 2.1)

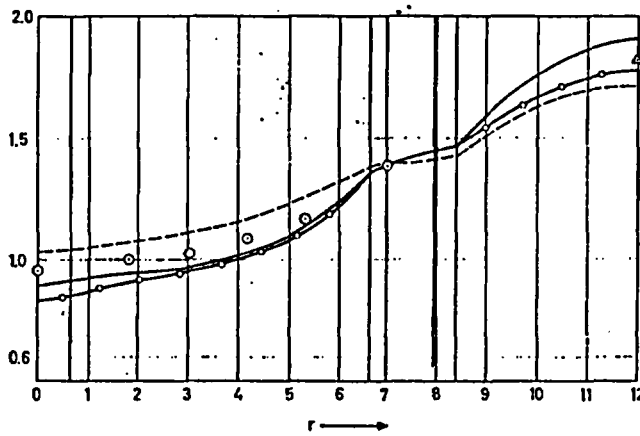


Fig. 8

Manganese reaction rate; Comparison of theory with experiment; Core 5001.

- 3-plus-40 group Carlson
- ARISTOS
- ..... 5-group Carlson
- Unmodified experimental values
- △ Modified experimental values  
(See section 2.1)

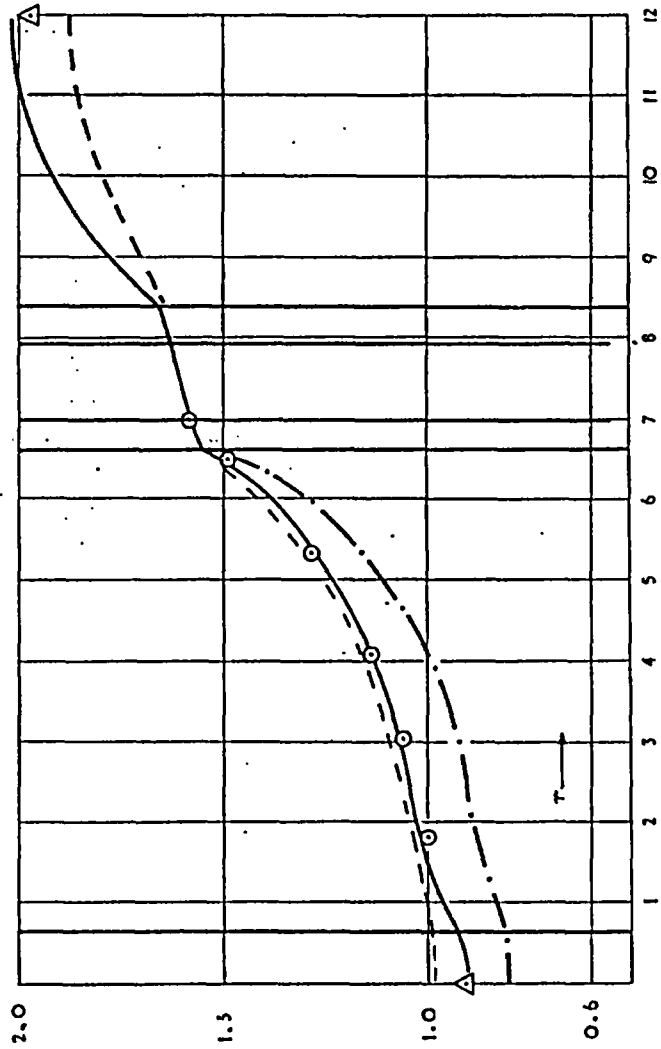


Fig. 9

Manganese reaction rate; Comparison of theory with experiment; Core 5002

- 3-plus-40 group Carlson
- - - ARISTOS
- · - · - 5-group Carlson
- Unmodified experimental values
- △ Modified experimental values  
(See section 2.1)

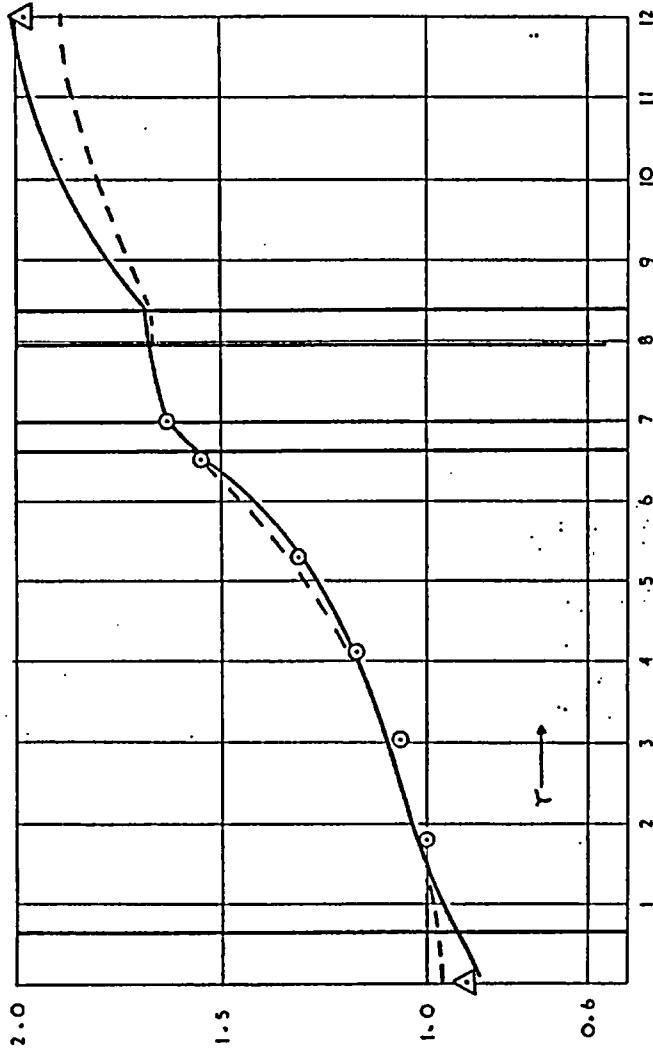


Fig. 10

Manganese reaction rate: Comparison of theory with experiment; Core 5003

- 3-plus-40 group Carlson
- - - ARISTOS
- Unmodified experimental values
- △ Modified experimental values  
(See section 2.1)

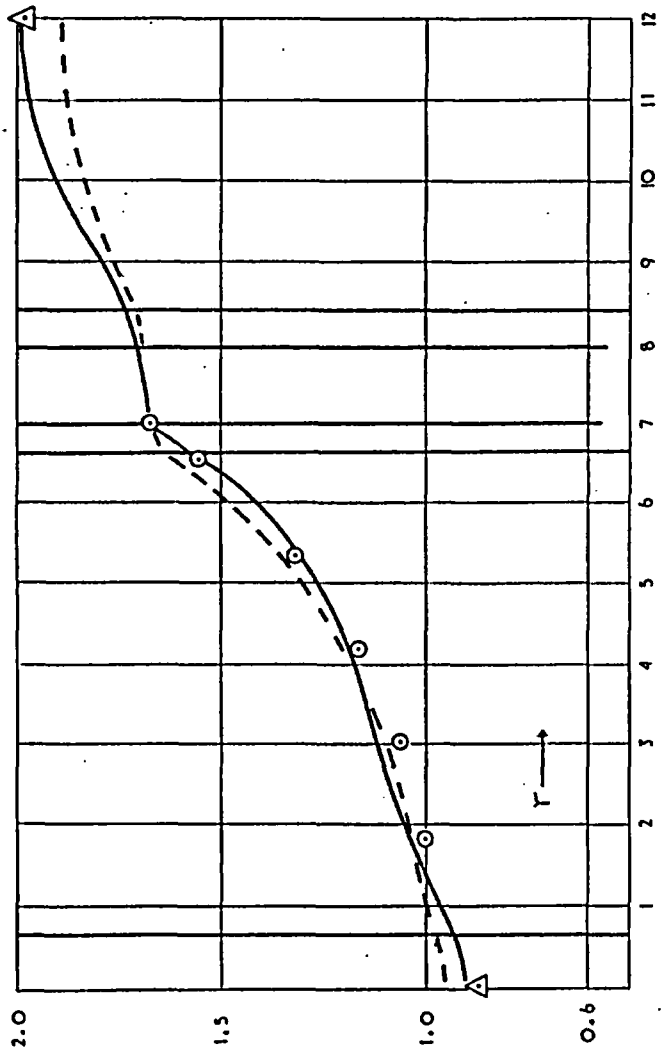


Fig. 11

Manganese reaction rate; Comparison of theory with experiment; Core 5004

- 3-plus-40 group Carlson
- - - ARISTOS
- Unmodified experimental values
- △ Modified experiment values (See section 2.1)

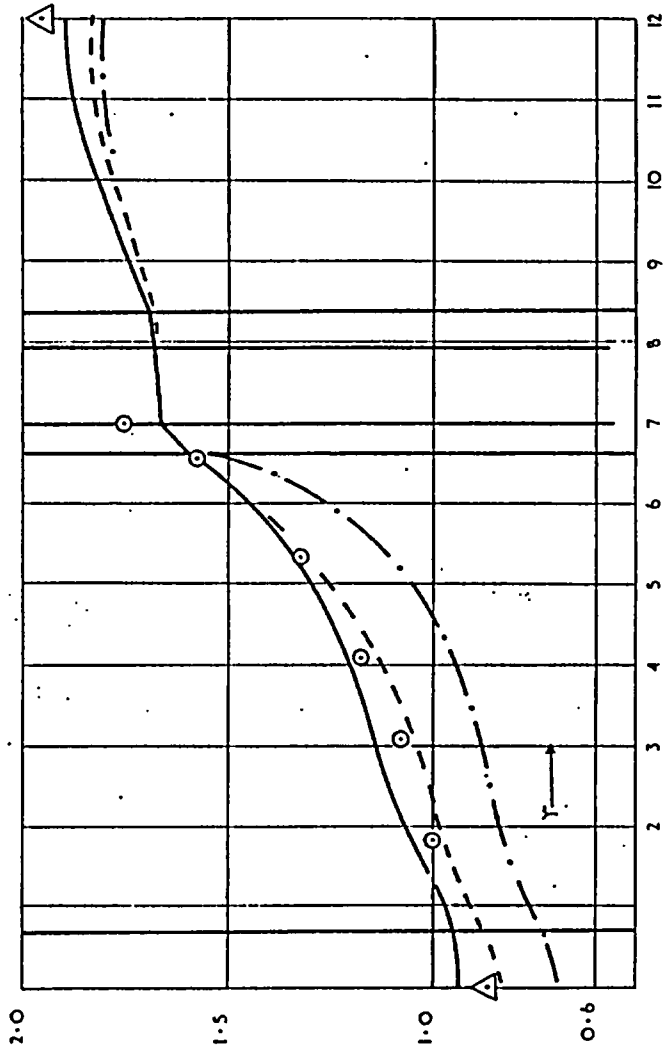


Fig. 12

Manganese reaction rate: Comparison of theory with experiment; Core 5005

- 3-plus-40 group Carlson
- - - - - ARISTOS
- · - · - 5-group Carlson
- Unmodified experimental values
- △ Modified experimental values (See section 2.1)

Some of this disagreement may be attributed to defects in the two-thermal-group spectrum model; to check this hypothesis, fine structure distributions given by the 3-plus-40-group Carlson calculations (see section 4.3) have also been plotted on Figs. 7 to 12. For the 100% D<sub>2</sub>O core (5002) the agreement between experiment and this "best" calculation is extremely good. LESLIE [13] has noted that a multi-thermal-group Carlson calculation using a free gas scattering law gives extremely good results in a CANDU lattice cell, which also contains only D<sub>2</sub>O.

As the percentage of light water in the coolant is increased, the theoretical fine structure becomes progressively too flat. It is known that the free gas scattering model does not reproduce properly the rise in the total scattering cross-section of H<sub>2</sub>O with diminishing energy. Therefore in these calculations the fuel cluster is too transparent at low energies. The use of better scattering laws for both H<sub>2</sub>O and D<sub>2</sub>O should improve the agreement with experiment. The source flux above 1.5 eV was assumed to be flat. Had it been assumed to vary across the cell in the same way as the group-3 flux, then the fine structure would be more pronounced and would show better agreement with experiment. However, as the group-3 flux extends down to 0.625 eV this would be an over-correction. The approxi-

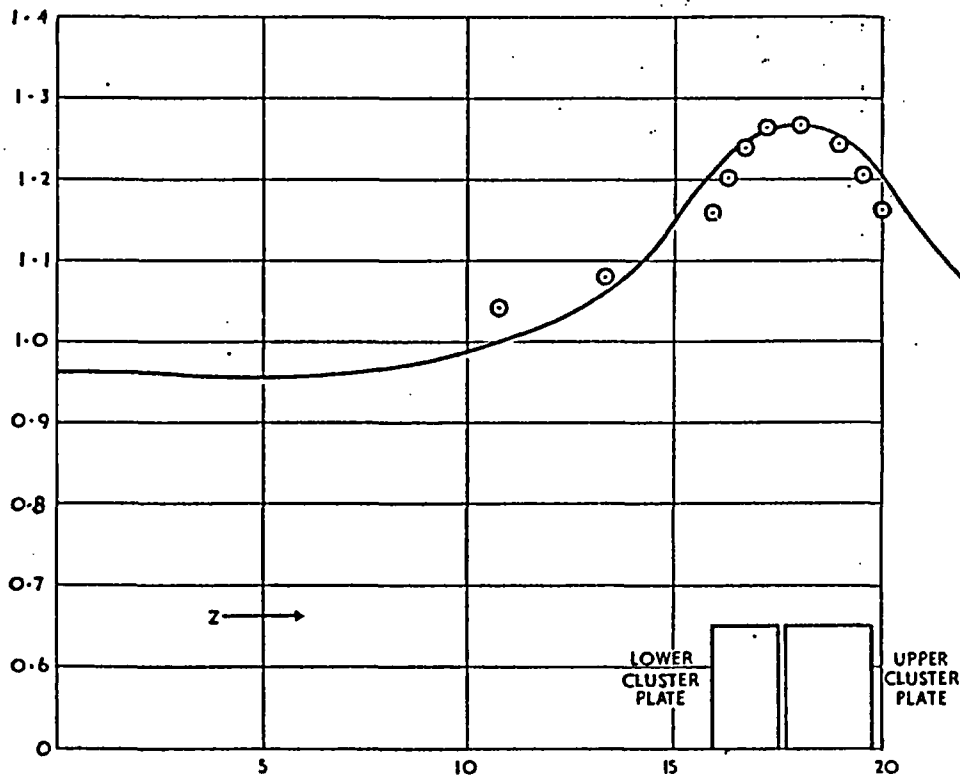


Fig. 13

Manganese axial reaction rate; Core 5001

— Angie computed values  
 ⊙ Experimental values

mation of using a uniform cluster may also be a little too crude. These three points are now under investigation, and it has been shown that a better representation of these effects does indeed greatly improve the agreement between calculated and measured fine structures. This work will be reported later.

In the air core (5001), the calculated fine structure is too steep. The same phenomenon has been noted in gas-cooled lattice cells, and it is attributed to the smearing model. The discrete fuel rods have been smeared into uniform fuel rings in both the Carlson and 5-group calculations. In the real geometry, neutrons can penetrate quite deeply into the cluster before encountering matter; in the equivalent uniform rings which are postulated in the calculation this is not so. Possible methods of representing this effect are now being investigated.

11.4. Axial distributions of manganese reaction rate

A comparison of the experimental values and the values computed with ANGIE [22] of the axial manganese reaction rates is shown in Figs. 13 to 16. Unfortunately, measurements were only made in the vicinity of the end-plates.

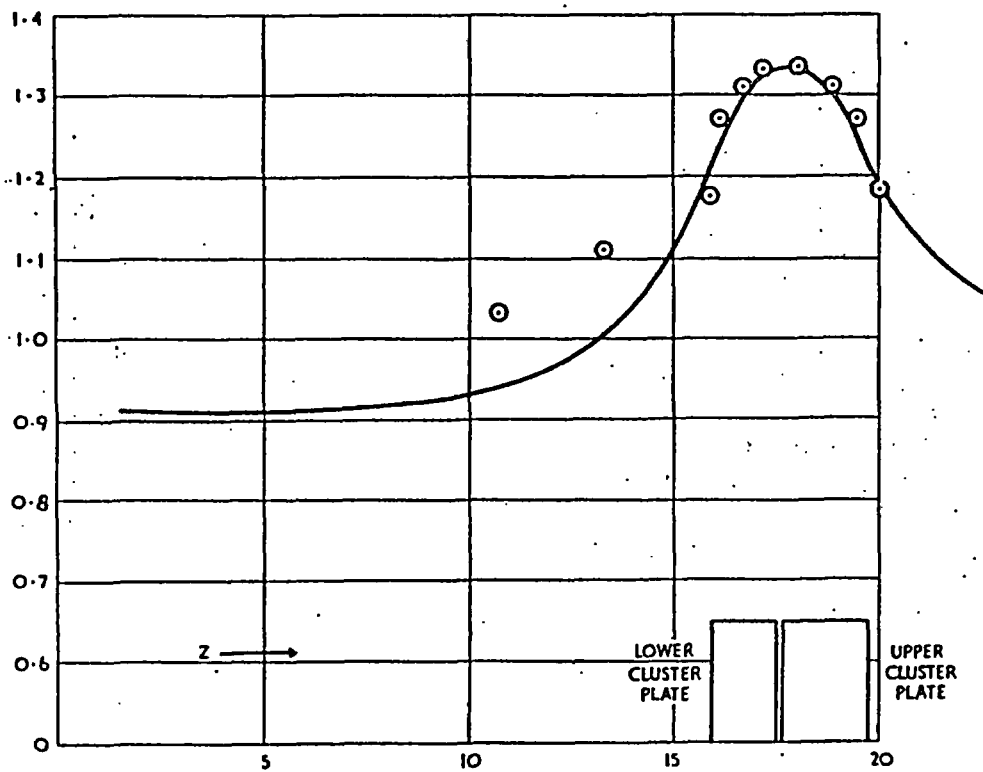


Fig. 14

Manganese axial reaction rate; Core 5002

— Angle computed values  
 ○ Experimental values

A  
f  
v.  
  
5  
l  
p  
o  
a  
  
1  
  
l  
c  
t  
r  
b  
d  
is  
  
31

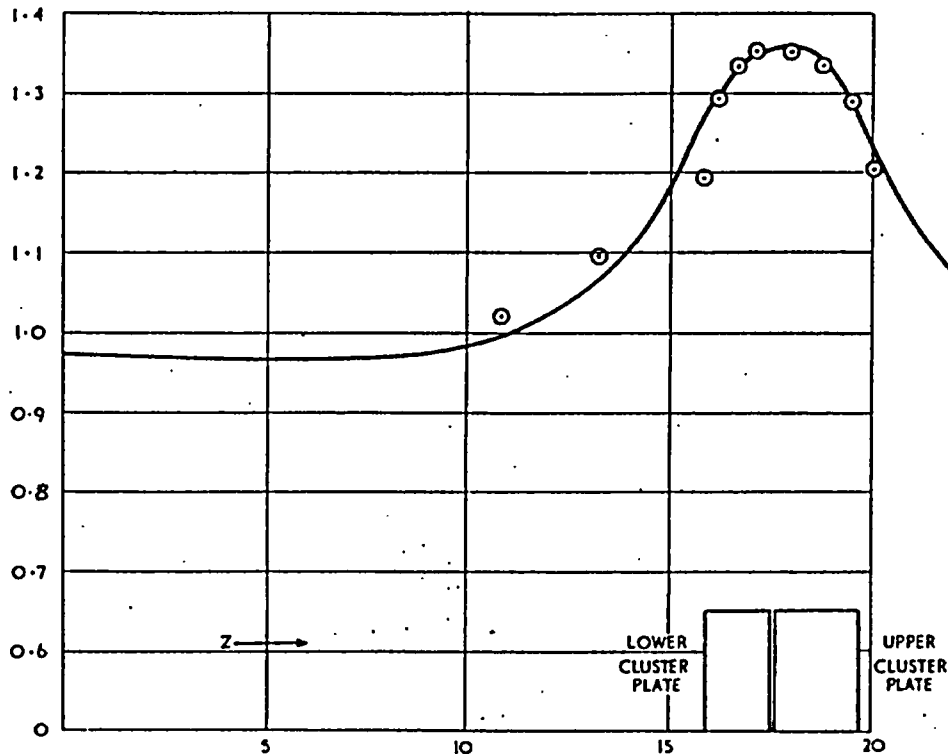


Fig. 15

Manganese axial reaction rate; Core 5004

— Angle computed values  
 ⊙ Experimental values

A few values near the mid-plane of the fuel pack would have been useful for normalizing the curves; as these values are lacking, the theoretical values were normalized to the peak experimental values.

The agreement between calculation and experiment is good in cores 5001 and 5004, though it is less satisfactory in core 5002. Since the calculations reported in section 5.1 show that the reactivity worth of the end-plates is relatively insensitive to the detailed flux distribution through them, one may be confident that ANGIE is computing this worth with adequate accuracy.

## 12. Spectrum indicators

Hyder and his co-workers made extensive measurements of the lutecium/manganese activation ratio as a function of position in the lattice cell for all five cores. This ratio alone does not suffice to determine the thermal spectrum. It was found that a theoretical model may predict this ratio correctly while getting other thermal reaction rates wrong. This may be understood in terms of the Westcott spectrum model. The Lu/Mn ratio depends mainly on  $T$  (the modal temperature of the best fit Maxwellian) and is relatively insensitive to  $r$  (the height of the epithermal tail). It had been

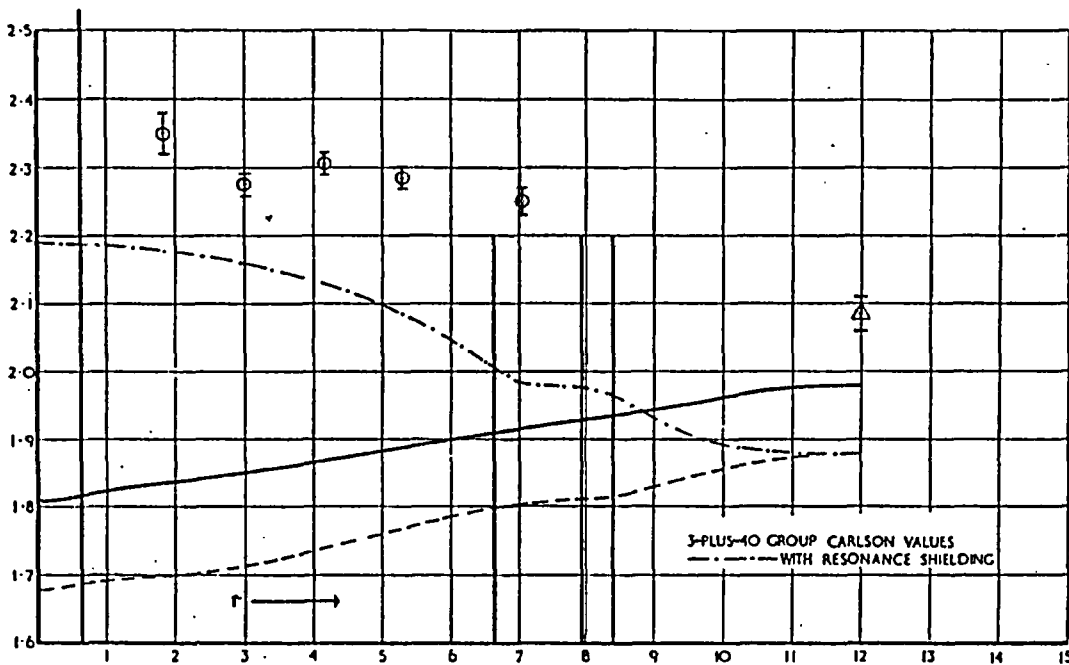


Fig. 16

Lutecium/Manganese reaction ratio; Core 5001

ARISTOS values { — Corrected for resonance shielding  
 - - - No resonance shielding  
 ○ Unmodified experimental values  
 △ Modified experimental values  
 (See section 2.1)

intended to supplement the Lu/Mn measurements with measurements of the  $\text{Pu}^{239}/\text{U}^{235}$  fission ratio, which would have fixed the thermal spectrum with much greater precision. Unfortunately, reactor time was so short that it was only possible to make a few such measurements.

### 12.1. Lutecium/manganese reaction-rate ratios

Cross-sections for lutecium-176 in the energy range 0 to 0.625 eV have been written into the SOFOCATE library. The same cross-sections have also been written into the 40-group library used in the Carlson calculations. These cross-sections were calculated from the published resonance parameters of J. P. ROBERGE and V. L. SAILOR [11]; an additional  $1/v$  cross-section of 23 b at 2200 m/s was added. These parameters are similar to those given by J. C. LISLE and A. S. G. TUCKEY [12]. These authors also give an experimental cross-section of  $2100 \pm 150$  b at 2000 m/s; the value in the SOFOCATE library is 1922 b. A group-3 cross-section of 106 b was used. This was derived from a  $1/v$  cross-section of 23 b at 2200 m/s together with a resonance integral of 950 b. As the effective thermal cross-sections are approximately 3000 b, this epithermal contribution is unimportant.

The spatial distributions of the lutecium/manganese reaction-rate ratios were calculated by means of the SANDPIPER/ARISTOS programmes and by the 40-group Carlson method. The 40-group Carlson values were corrected for the epithermal effects by multiplying by the ratio of total reaction ratio to thermal reaction ratio as calculated by the 5-group Carlson method. The theoretical values were normalized so as to make the reaction-rate ratio in a room temperature Maxwellian equal to 1.748. Since this is the ratio measured for the experimental foil, these normalized theoretical values may be compared directly with the experiments. The experimental values along the cell boundary were interpolated using the Cohen method (see section 11).

HYDER, KENWARD and PRICE [14] argue that there is considerable resonance shielding in the manganese foils and that the epithermal cross-section should be divided by a factor of 1.38. The theoretical values have been plotted with and without this correction. It will be seen from Figs. 16 to 20, that this correction has a considerable effect on the absolute value of the Lu/Mn ratio, though not so much on its distribution.

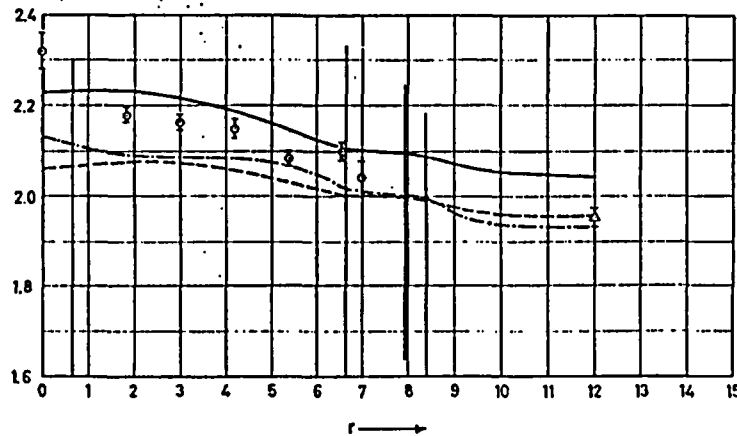


Fig. 17

Lutecium/Manganese reaction ratio; Core 5003

- Unmodified experimental values
- △ Modified experimental values
- Corrected for resonance shielding
- No resonance shielding
- 3-plus-40 group Carlson values with resonance shielding

With the exception of the air core (5001), the ARISTOS and Carlson values are quite close, and both are in good agreement with the experiments. If no correction is made for resonance self-shielding the ARISTOS values tend to be too high, implying that the spectrum model is too hard. The Carlson values tend to be too low, suggesting that the spectrum model used in these multi-thermal-group calculations is too soft. This confirms the findings of more basic studies that the free gas model of thermalization is considerably too soft for both  $H_2O$  and  $D_2O$ .

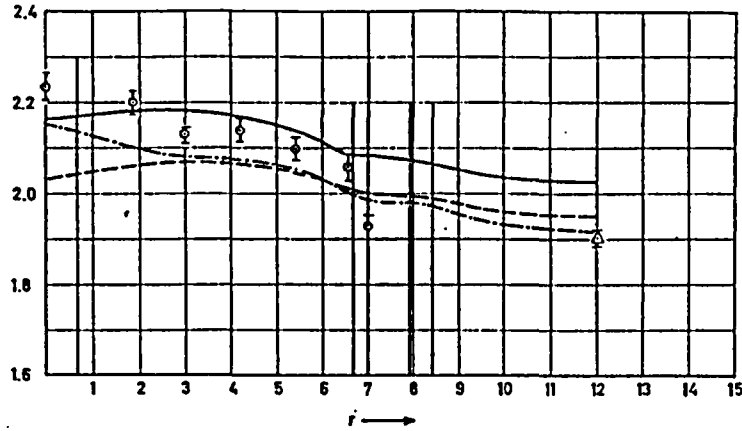


Fig. 18

Lutesium/Manganese reaction ratio; Core 5003

- Unmodified experimental values
  - △ Modified experimental values  
(See section 2.1)
- ARISTOS values {
- Corrected for resonance shielding
  - - - No resonance shielding
  - · - · 3-plus-40 group Carlson values with resonance shielding

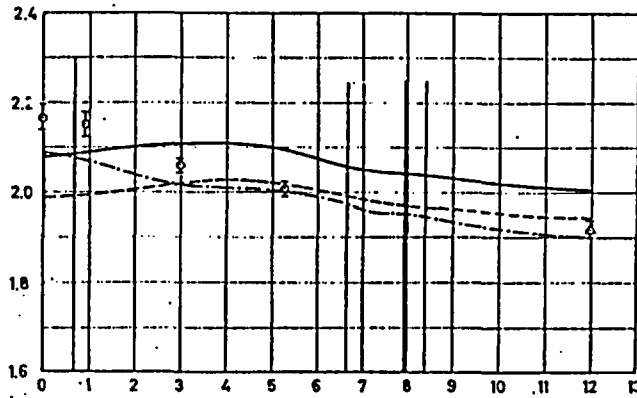


Fig. 19

Lutesium/Manganese reaction ratio; Core 5004

- Unmodified experimental values
  - △ Modified experimental values  
(See section 2.1)
- ARISTOS values {
- Corrected for resonance shielding
  - - - No resonance shielding
  - · - · 3-plus-40 group Carlson values with resonance shielding

In the air core both models are much too soft, the ARISTOS results being further from the experimental points than the Carlson values. The behaviour of the Carlson calculations is readily comprehensible, since it

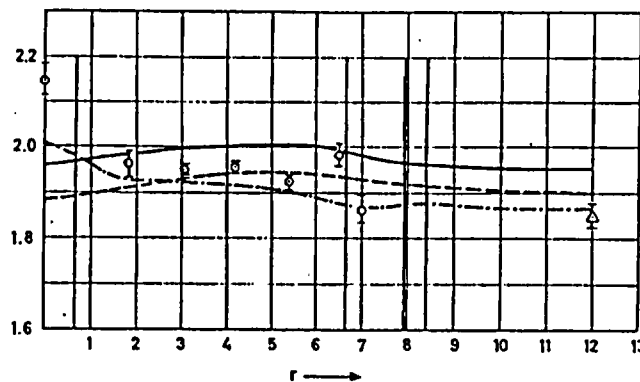


Fig. 20

Lutecium/Manganese reaction ratio; Core 5005

- Unmodified experimental values
- Δ Modified experimental values (See section 2.1)
- ARISTOS values {
  - Corrected for resonance shielding
  - - - No resonance shielding
  - · - 3-plus-40 group Carlson values with resonance shielding

is known that the free gas model of thermalization is too soft, and it is to be expected that the resulting discrepancies with experiment will be greatest in the most under-moderated core. Later work, which will be reported separately has shown that the use of an improved Scattering Law, derived from the Chalk River experiments, improves the agreement between theory and experiment on such spectrum-sensitive parameters.

The poor results of the 5-group scheme for the air core are also in accordance with expectation. In this core the group-4 spectrum has to be switched out, (see Reference [2] ) and the thermal spectrum model is therefore much poorer than in the other 4 cores. The new iterative version of METHUSELAH (see section 10.2) avoids this switching out of group 4 and gives much better results in the air core (this work will be reported separately).

### 12.2. Plutonium-239/uranium-235 fission ratios

This ratio has been measured at position  $d_3$  ( $r = 4.188$  cm) in cores 5002, 5004 and 5005 only.

Fission ratios have been calculated both by the ARISTOS method and by the 3+40-group Carlson method. The 40-group Carlson flux was normalized so that the total absorption was equal to the group-3 removal given by the 5-group Carlson calculation. The theoretical values were normalized so that the fission ratio in a 20°C Maxwellian was equal to 1.077, the value measured for the fission chamber pair used in the experiments. These normalized theoretical values are therefore directly comparable with the experimental numbers.

Table XXVI shows the comparison of theory with experiment. It will be seen that there is fairly good agreement between the Carlson and the

TABLE XXVI

## COMPARISON OF PLUTONIUM-239/URANIUM-235 FISSION-RATE RATIOS

Core	Pu <sup>239</sup> /U <sup>235</sup> fission ratios		
	ARISTOS	Carlson	Experiment
Maxwellian (20°C)	1.077	1.077	1.077
5002	1.704	1.550	1.520
5004	1.457	1.345	1.375
5005	1.325	1.277	1.266

experimental values, showing that there is no basic theoretical uncertainty in the spectrum at this position. The two-thermal-group method, however, overestimates the ratio by as much as 12%. These discrepancies must be due to the two-thermal-group model miscalculating the Westcott r-value in the fuel. The good agreement on the lutecium/manganese ratio shows that the two-thermal-group model is calculating Westcott's parameter T quite accurately.

### 13. Ratios of U<sup>238</sup> fission rates to U<sup>235</sup> fission rates

The experimental values of the U<sup>235</sup> fission rates and the ratios of U<sup>238</sup> to U<sup>235</sup> fission rates were measured by Fox and others (unpublished). The U<sup>235</sup> fission rates have been normalized to unity for the first fuel ring. The fission-rate ratios are absolute, that is, they are the ratios of fissions per atom.

The methods by which the fission-rate distributions are calculated are described in section 6.3. These calculations will now be compared with the experimental measurements. Figs. 21 to 23 show a comparison of the experimental and theoretical (3 plus 40-group Carlson only) values of U<sup>235</sup> fission rates for cores 5001, 5002 and 5005. It will be seen that the trend of the results is consistent with those found for the manganese reaction-rate distributions. (This is to be expected, since U<sup>235</sup> is almost a 1/v detector). The theoretical fine structure is too steep in the air core, is very nearly correct in the D<sub>2</sub>O core, and is too flat in the H<sub>2</sub>O core.

The values of  $\delta_{28}$ , the ratio of U<sup>238</sup> fissions to U<sup>235</sup> fissions, for the whole fuel bundle are given in Table XXVII.

A comparison of the fission-rate ratio distributions is given in Figs. 24 to 28.

It will be seen that the Carlson fission ratios are considerably nearer to the experimental ratios than are the ARISTOS values. The improvement is due to the higher group 1 flux in the fuel given by the 5-group Carlson calculations. In group 1 the mean free paths are long — of the order of 10 cm — and the transport corrections to diffusion theory are large. These

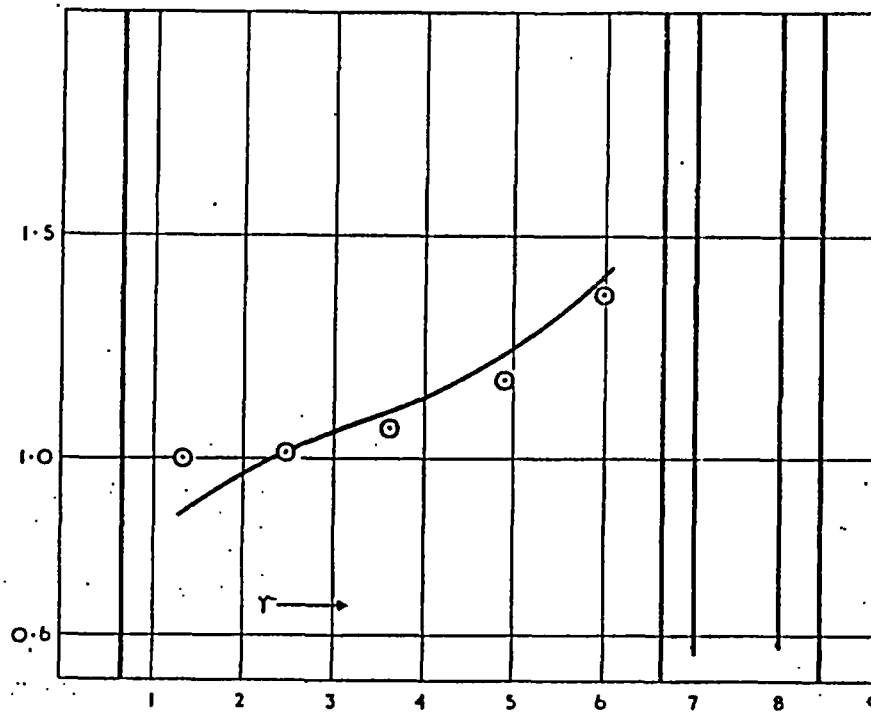


Fig. 21

$U^{235}$  fission rate; Comparison of theory with experiment; Core 5001

— Theoretical curve  
 ○ Experimental values  
 3-plus-40 group Carlson

TABLE XXVII

$U^{238}/U^{235}$  FISSION RATIOS

Core	$\delta_{28}$ (whole fuel bundle)		
	Expt.	ARISTOS	Carlson
5001	0.0647	0.0427	0.0571
5002	0.0461	0.0327	0.0386
5003	0.0544	0.0318	0.0373
5004	0.0504	0.0309	0.0366
5005	0.0458	0.0298	0.0358

corrections always tend to increase the flux peaking. Since in group 1 the sources are in the fuel, the correction increases the flux in the fuel.

Day and others (unpublished) have calculated the  $U^{238}$  fission rates in cores 5001, 5002, and 5005 using the multi-group Monte Carlo code SPEC [15]. The neutron source in this calculation is taken from the experimentally:

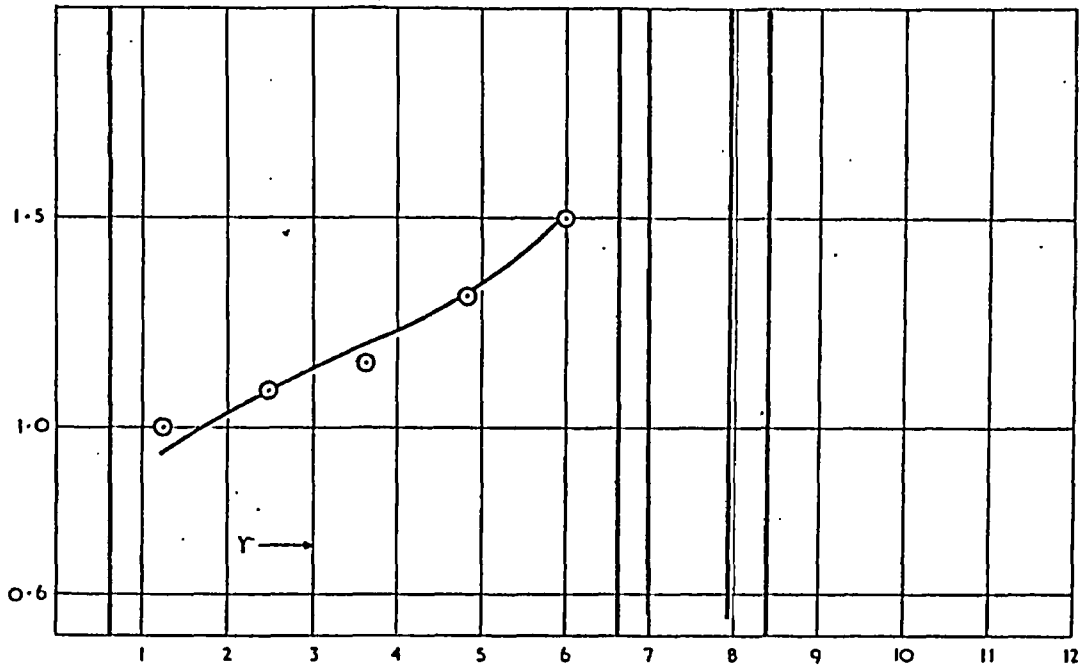


Fig. 22

$U^{235}$  fission rate; Comparison of theory with experiment; Core 5002

— Theoretical curve  
 ○ Experimental values  
 3-plus-40 group Carlson

measured distribution of  $U^{235}$  fission rates, and this experimental distribution is also used to give the fission ratio. The SPEC and Carlson calculations agree reasonably well in core 5001 and extremely well in cores 5002 and 5005. This suggests that the discrepancy between theory and experiment is due to errors in data rather than in the solution of the transport equation. (Since the experiment is an extremely difficult one, the possibility of experimental error must also be considered). Indeed, evidence is now accumulating (see Reference [22]) that the inelastic scattering cross-section of  $U^{238}$  in the resonance region may have been overestimated.

The discrepancies revealed in Table XXVII have a considerable effect on reactivity. This is discussed in section 15 below.

#### 14. The ratio of epi-cadmium to hypo-cadmium capture in $U^{238}$

The ratios of epi-cadmium to hypo-cadmium capture (that is, the ratio of capture above the Cd cutoff to capture below this cutoff) in  $U^{238}$  have also been measured by Fox and co-workers (unpublished). Unfortunately, in all but two cases, metal guard foils were used. It is generally agreed that this has invalidated the measurements, and no method has been discovered of correcting for the effect of these guard foils.

A comparison between theory and experiment has been made for the two cases in which oxide guard foils were used. These are the innermost and outermost fuel rings of core 5004. The capture ratio was computed

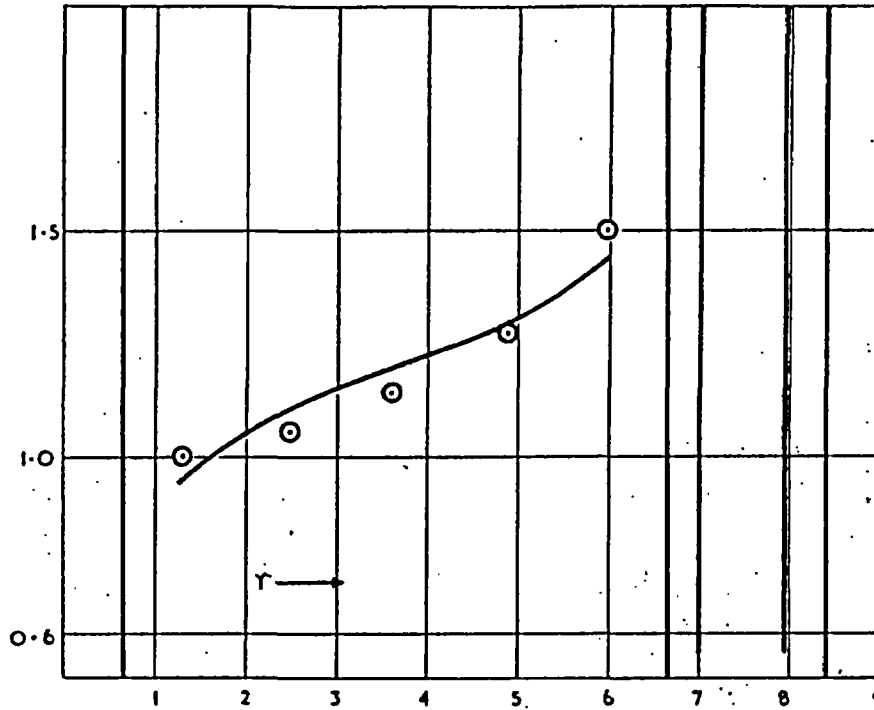


Fig. 23

$U^{235}$  fission rate; Comparison of theory with experiment; Core 5005

— Theoretical curve  
 ○ Experimental values  
 3-plus-40 group Carlson

by the 3-plus-40 group Carlson method described in sections 4.3 and 4.4. A MOCUP Monte Carlo calculation was used to correct the  $U^{238}$  absorption in group 3; this process is described in section 4.4. The expression for the capture ratio is

$$\rho_{28} = \frac{\Phi_1 \sigma_{c1} + \Phi_2 \sigma_{c2} + \Phi_3 \sigma_{c3} + Y}{W_f \sigma_{ct}^{28} \phi_t - Y}$$

where  $Y$  is the  $U^{238}$  capture between the cadmium cut-off energy and 0.625 eV;

$W_f$  is the hyperfine flux weighting factor for the fuel.

The comparison of theoretical and experimental results is given in Table XXVIII. It will be seen that the theoretical ratio is insensitive to the choice of cadmium cut-off energy.

It will be seen that the theoretical values are larger than the experimental values. The reason for this discrepancy is not known. However,

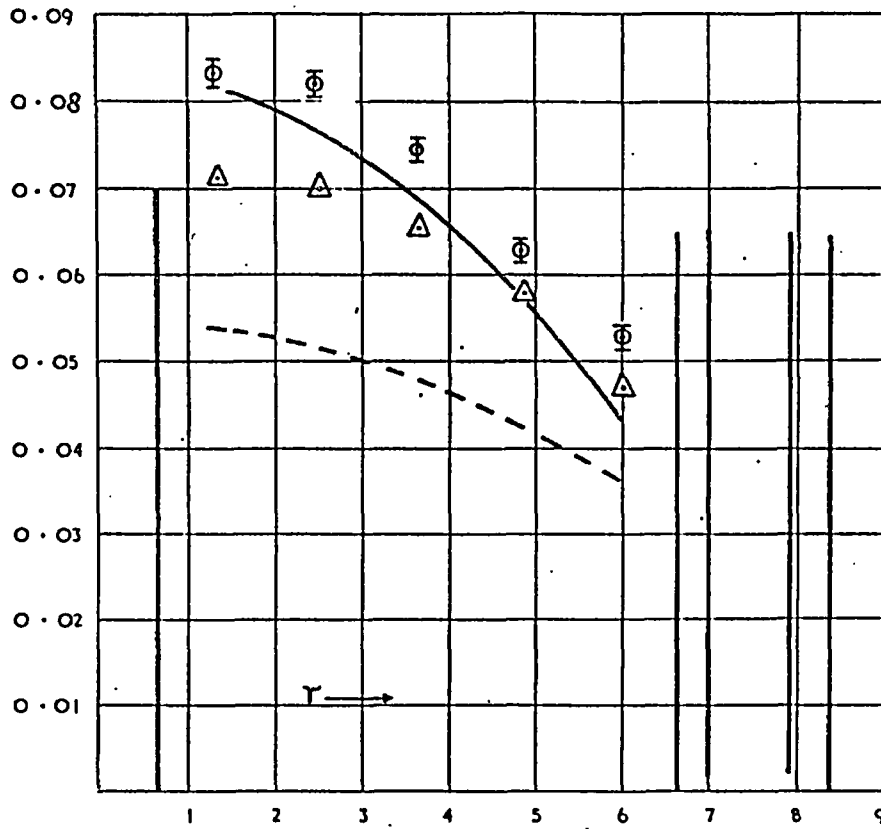


Fig. 24

Ratio of  $U^{238}$  fission rate to  $U^{235}$  fission rate; Comparison of theory with experiment; Core 5001

- 40-plus-3 group Carlson
- - - ARISTOS
- Φ Experimental values
- Δ Spec.values

TABLE XXVIII

COMPARISON OF EPI-CADMIUM TO HYPO-CADMIUM  $U^{238}$  CAPTURE RATIOS: CORE 5004

Fuel ring	$\rho_{28} = \frac{(\text{epi-cadmium capture})}{(\text{hypo-cadmium capture}) U^{238}}$		
	Expt.	Theory (using cut-off at 0.4 eV)	Theory (using cut-off at 0.625 eV)
1	1.203	1.408	1.309
5	0.896	1.041	0.981

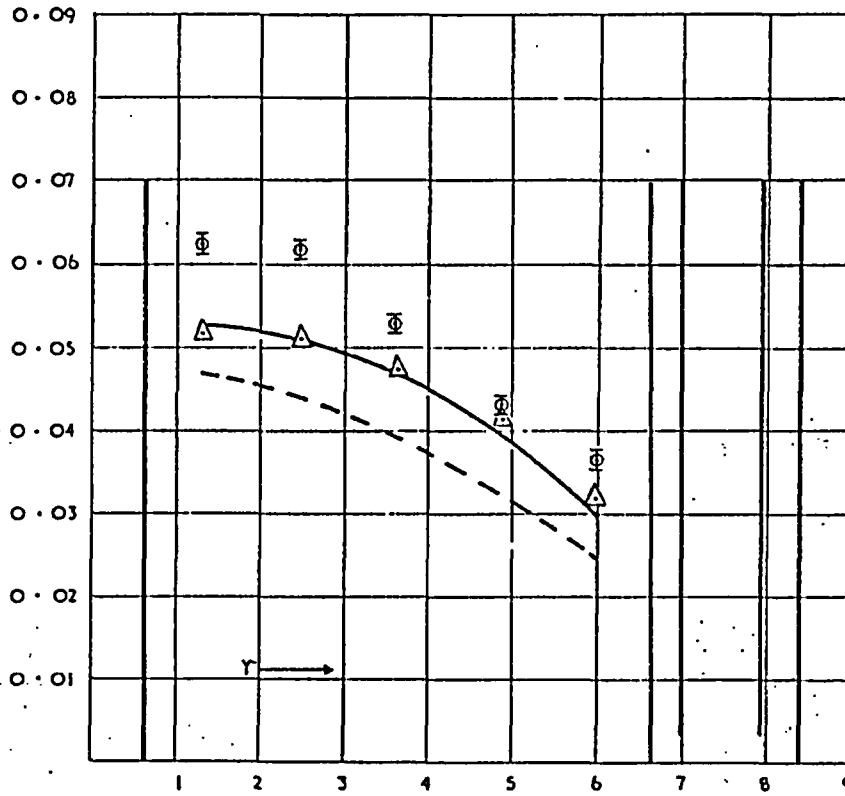


Fig. 25

Ratio of  $U^{238}$  fission rate to  $U^{235}$  fission rate; Comparison of theory with experiment; Core 5002

- 40-plus-3 group Carlson
- - - ARISTOS
- ⊕ Experimental values
- Δ Spec. values

it should be remembered that the use of cadmium in resonance escape measurements is now regarded with suspicion, particularly in  $H_2O$  systems. (The coolant in core 5004 contains 40%  $H_2O$ ). Therefore it should not necessarily be assumed that the theoretical calculations are wrong.

### 15. Experimental corrections to reactivity

The calculated reaction rates do not all agree with experiment. The effects of the discrepancies on reactivity will now be discussed.

#### 15:1. The effect of fine structure discrepancies on reactivity

The theoretical radial distributions of manganese reaction rate show discrepancies with experiment. The method of calculating the effect of these discrepancies on the reactivity is explained below.

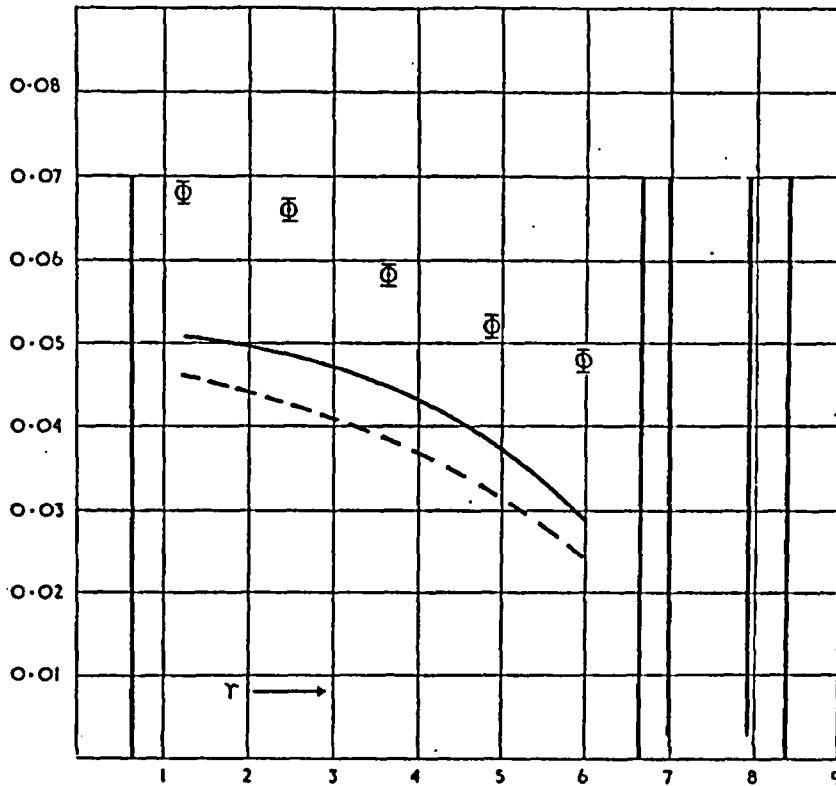


Fig. 26

Ratio of  $U^{238}$  fission rate to  $U^{235}$  fission rate; Comparison of theory with experiment; Core 5003

— 3-plus-40 group Carlson  
 - - - ARISTOS  
 \* Experimental values

Let " $q_j$ " be the fraction of thermal neutrons absorbed in region  $j$ . Then as the absorption cross-sections have approximately a  $1/v$  dependence on energy, we have:-

$$\left(\frac{q_j}{q_{\text{fuel}}}\right)_{\text{expt}} \approx \left(\frac{q_j}{q_{\text{fuel}}}\right)_{\text{theory}} \cdot \frac{(\text{Mn reaction rate, } j)_{\text{expt.}}}{(\text{Mn reaction rate, } j)_{\text{theory}}} \cdot \frac{(\text{Mn reaction rate, fuel})_{\text{theory}}}{(\text{Mn reaction rate, fuel})_{\text{expt.}}}$$

and

$$\frac{1}{q_{\text{fuel}}} - 1 = \frac{q(\text{tie rod})}{q(\text{fuel})} + \frac{q(\text{cal. tube})}{q(\text{fuel})} + \frac{q(\text{press. tube})}{q(\text{fuel})} + \frac{q(\text{mod.})}{q(\text{fuel})}$$

The thermal utilization  $f$  is then obtained by multiplying together  $q_{\text{fuel}}$  and the probability that a neutron which is absorbed in the fuel will be absorbed in  $U^{235}$  rather than in  $U^{238}$ . This latter quantity is independent of thermal fine structure.

The resulting reactivity discrepancies are given in Table XXIX.

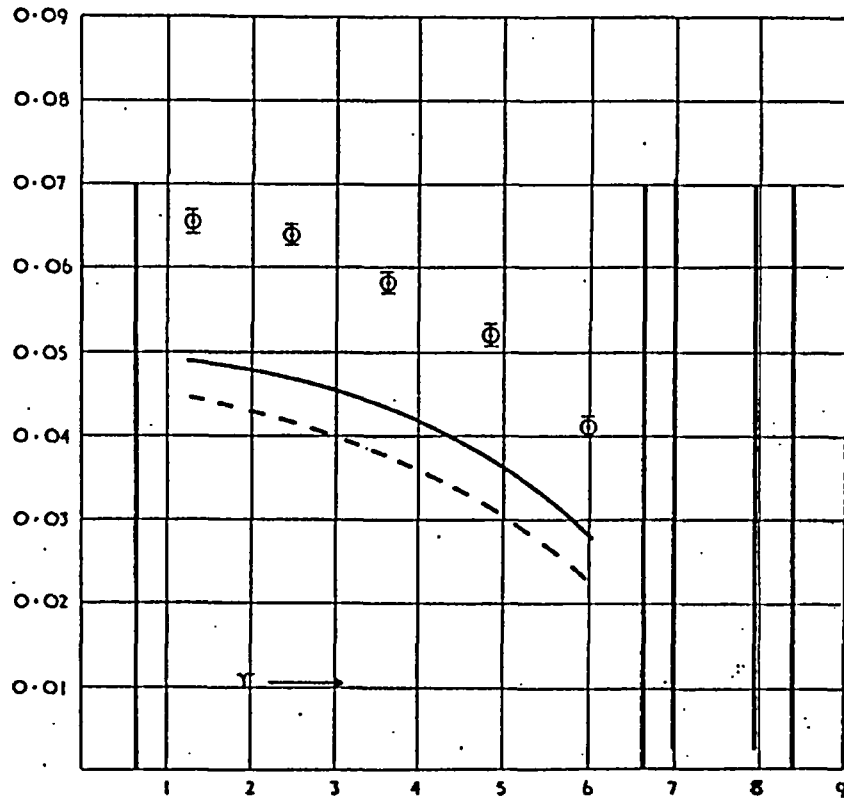


Fig. 27

Ratio of  $U^{235}$  fission rate to  $U^{238}$  fission rate; Comparison of theory with experiment; Core 5004

——— 3-plus-40 group Carlson  
 - - - - - ARISTOS  
 φ Experimental values

TABLE XXIX

REACTIVITY CORRECTIONS OBTAINED FROM MANGANESE REACTION RATES

Core	Experiment $q_{fuel}$	Theory $q_{fuel}$	$\Delta k$
5001	0.9091	0.9074	+0.17%
5002		0.9068	negligible
5003		0.9105	negligible
5004	0.9116	0.9137	-0.22%
5005	0.9158	0.9217	-0.61%

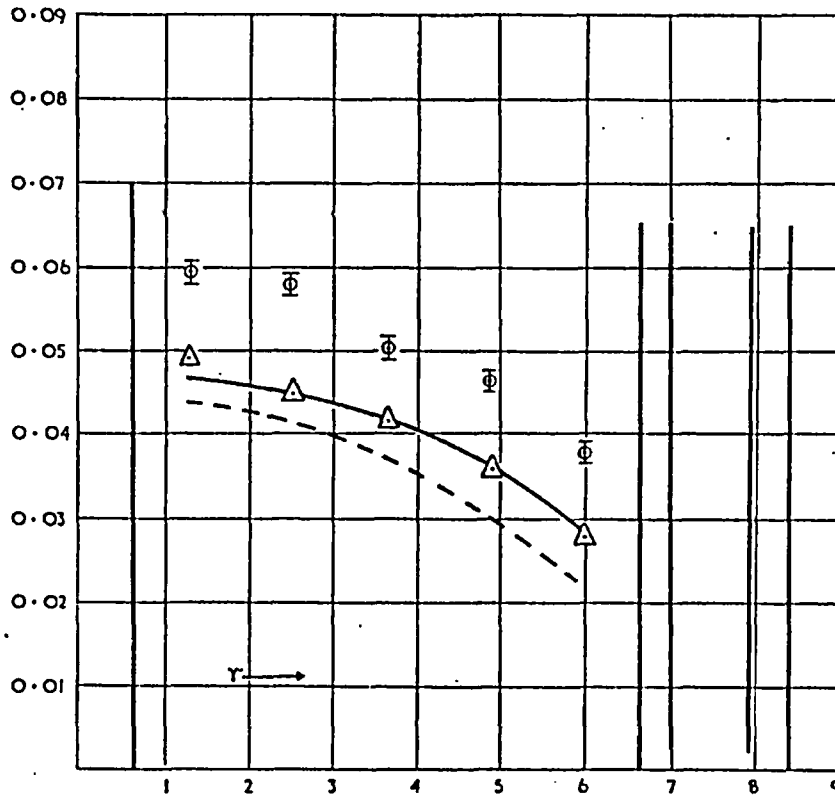


Fig. 28

Ratio of  $U^{235}$  fission rate to  $U^{235}$  fission rate; Comparison of theory with experiment; Core 5005

——— 3-plus-40 group Carlson  
 - - - - - ARISTOS  
 $\phi$  Experimental values.  
 $\Delta$  Spec. values

These corrections are only approximate; it was difficult to interpret the experimental values as there are so few of them. The large correction for core 5005 arises from the large rise in the experimental reaction rate across the pressure tube. This experimental result is dubious. The discrepancies between theory and experiment for cores 5002 and 5003 were negligible.

### 15.2. The effect of Lu/Mn reaction-rate discrepancies on reactivity

It is only in core 5001 that the discrepancy is large enough to produce an appreciable change in reactivity. In this core, the theoretical spectrum is too soft. Hardening the spectrum will reduce the ratio of  $U^{235}$  absorption to  $1/v$  absorption. Thus the thermal utilization will decrease. This effect, assuming all other materials in the cell have a  $1/v$  dependence, is approximately given by

$$\frac{\delta f_{25}}{f_{25}} = (1 - f_{25}) \frac{\delta[\sigma_{25}/(1/v)]}{\sigma_{25}/(1/v)}$$

One possible method of interpreting the discrepancy is to treat the fuel spectrum as a temperature-hardened Maxwellian. The experimental measurement of the Lu/Mn ratio can then be interpreted as a determination of the mean Westcott  $g$ -factor of Lu-176 in the fuel

$$g_{Lu}(\text{fuel}) = \frac{(Lu/Mn)_{\text{fuel}}}{\sigma_0(Lu)/\sigma_0(Mn)},$$

the suffix 0 indicating a 2200 m/s cross-section. The temperature of the equivalent Maxwellian is just that  $T$  which makes  $g_{Lu}(T)$  in Westcott's table equal to the measured value. A theoretical temperature may be defined in exactly the same way. Then

$$\delta f_{25}/f_{25} \approx (1 - f_{25}) \{ g_{a5}(T_{\text{expt.}}) - g_{a5}(T_{\text{theory}}) \}.$$

This correction reduces the reactivity by about 0.20%. The consequent change in  $\eta_5$  contributes less than 0.1% and has been ignored.

Another possible method of correction is to take as the adjustable parameter the amount of  $1/v$  absorption in a Wigner-Wilkins spectrum formed at room temperature. This gives a reactivity correction of -0.30%, and a mean value of -0.25% has therefore been adopted. In the absence of a complete set of Pu/U fission ratio measurements, it is not possible to make a proper 2-parameter adjustment of the theoretical spectrum.

### 15.3. The effect of $U^{238}/U^{235}$ fission ratio discrepancies on reactivity

The method of correcting reactivity for  $U^{238}/U^{235}$  fission ratio discrepancies has already been discussed in section 6.3. Table XXX shows the reactivity differences between theory and experiment for each of the cores. For comparison the differences between ARISTOS and the Carlson predictions are repeated.

TABLE XXX

#### EFFECT OF FISSION RATIO DISCREPANCIES ON REACTIVITY

Core	$\Delta k$ ( $U^{238}$ fission; Carlson-ARISTOS)	$\Delta k$ ( $U^{238}$ fission; Expt. -Carlson)
5001	+1.52%	+0.79%
5002	0.63%	0.80%
5003	0.59%	1.81%
5004	0.61%	-1.47%
5005	0.64%	1.07%

It will be seen that the change in reactivity due to the fission ratios calculated by the Carlson method and by ARISTOS are approximately equal to the differences in  $(\eta f)_f$  as calculated by the 5-group Carlson and by ARISTOS, (see Table XVIII).

#### 15.4. Total experimental corrections to reactivity

Table XXXI summarizes the experimental reaction-rate corrections to reactivity. (In the absence of suitable measurements, no correction can be made for resonance capture in  $U^{238}$ ). It will be seen that this correction produce a considerable improvement.

TABLE XXXI

#### EXPERIMENTAL REACTION-RATE CORRECTIONS TO $k_{eff}$

Core	5001	5002	5003	5004	5005
$\Delta k \frac{(U^{238} \text{ fiss})}{(U^{235} \text{ fiss})}$	+0.79%	+0.80%	+1.81%	+1.47%	+1.107%
$\Delta k$ (Lu/Mn)	-0.25%	0	0	0	0
$\Delta k$ (Mn fine structure)	+0.17%	0	0	-0.22%	-0.61%
$k_{eff}$ (theory)	0.9956	0.9825	0.9824	0.9849	0.9934
$k_{eff}$ (corrected)	1.0027	1.0005	1.0005	0.9974	0.9980

The same corrections have been applied to the theoretical values of  $k_{inf}$ . Table XXXII shows a comparison of these corrected values with the experimental values listed in Table XXIV.

TABLE XXXII

#### EXPERIMENTAL REACTION-RATE CORRECTIONS TO $k_{inf}$

Core	$k_{inf}$ (experimental)	$k_{inf}$ (theory) with reaction-rate corrections
5001	1.0302	1.0322
5002	1.0329	1.0325
5003	1.0435	1.0434
5004	1.0454	1.0422
5005	1.0075	1.0055

It will be seen that the discrepancies between the theoretical and experimental values of  $k_{inf}$  are almost the same as the discrepancies between the values of  $k_{eff}$  and unity. This is to be expected in these relatively low-buckling cores.

The agreement between the experimental  $k_{inf}$  and the theoretical  $k_{inf}$  with corrections for experimental reaction-rate distributions is staggeringly good: the maximum discrepancy in Table XXXII is 0.32%. Since the experimental  $k_{inf}$  is calculated using theoretical leakages, one may conclude either (i) that the nuclear data, the calculation of resonance escape and the calculation of leakage are all satisfactory to this accuracy, or (ii) that there are errors in these quantities which cancel out in all five cores.

In order to decide between these alternatives, it will be necessary to analyse a much wider range of cores.

## 16. Conclusions

The reactivities and reaction rates obtained measured in a series of experiments on pressure-tube heavy water cores in Dimple have been compared with Carlson Sn and Monte Carlo calculations. With the exception of the air core, there is good agreement between the theoretical and experimental values of the lutecium/manganese reaction ratio. There is also good agreement with the  $Pu^{239}/U^{235}$  fission ratios. The predictions of the  $U^{238}/U^{235}$  fission-rate ratios are poor. The predictions of manganese fine structure are good in the case of the 100%  $D_2O$  but less satisfactory for the air and  $H_2O$  cores. The measures which are being taken to remedy this discrepancy are described in section 11.3. Also the theoretical predictions of reactivity are all low. The reaction-rate discrepancies and reactivity discrepancies are, however, consistent: if the reaction-rate discrepancies are used to correct the theoretical reactivities, then there is excellent agreement between these corrected reactivities and the experimental values.

The predictions of the 5-group scheme (as realized in the SANDPIPER III and ARISTOS programmes) have been compared with both the experiments and the results of more sophisticated calculations. The raw ARISTOS output must be corrected for such things as the effect of end-fittings, and the corrected eigenvalues and  $k_{inf}$  are in reasonable agreement with experiment (except for the air core). A detailed comparison between the 5-group computations and the sophisticated calculations shows that this agreement is to some extent fortuitous, being due to the cancelling effect of a number of small errors. However, the value of the 5-group scheme for assessment and survey purposes is confirmed by this study.

Obviously much more work is required to resolve the discrepancies between theory and experiment which this study has revealed; while the discrepancies remain, a report such as this is, in some sense, incomplete. There will always be reasons for delaying publication so that yet another improvement in theory can be incorporated. It is felt that the time has come to publish the results obtained so far. Investigations on these lines are continuing.

## ACKNOWLEDGEMENTS

The author wishes to thank Mr. M. J. Terry and Mr. M. J. Roth for their assistance in performing Carlson calculations, Dr. C. T. Chudley, Dr. W. N. Fox and Mr. D. H. Day for making available the SPEC calculations, and Mr. A. J. Briggs for performing the MOCUP calculations. In particular the author wishes to acknowledge the advice given by Dr. D. G. Leslie throughout the whole of this study.

## APPENDIX I

## THE DIMENSIONS OF THE LATTICES

Fuel	1.605 Co, UO <sub>2</sub>
Pellet radius	0.3797 cm
Inner radius of	
Aluminium clad	0.3886 cm
Clad thickness	0.09144 cm
Radius of 1st fuel ring	1.321 cm
Radius of 2nd fuel ring	2.489 cm
Radius of 3rd fuel ring	3.658 cm
Radius of 4th fuel ring	4.851 cm
Radius of 5th fuel ring	6.020 cm
Number of rods on 1st ring	6
Number of rods on 2nd ring	12
Number of rods on 3rd ring	18
Number of rods on 4th ring	24
Number of rods on 5th ring	30
Radius of steel tie rod	0.635 cm
Inner radius of pressure tube	6.6599 cm
Outer radius of pressure tube	6.985 cm
Inner radius of calandria tube	7.926 cm
Outer radius of calandria tube	8.414 cm
Lattice pitch	21.2725 cm, square
Bulk moderator	99.7% D <sub>2</sub> O

## APPENDIX 2

## THE CROSS-SECTIONS USED IN SANDPIPER AND THE FORTY-GROUP CARLSON CALCULATIONS

The SANDPIPER III library is based on a compilation of SOFOCATE computed values compiled by H. J. AMSTER [4]. These cross-sections were renormalized to the world consistent set of 2200 m/s cross-

TABLE XXXIII

COMPARISON OF 2200 m/s CROSS-SECTIONS USED IN SANDPIPER  
AND THE 40-GROUP CARLSON CALCULATIONS

Parameter	World Consistent set Supplement No. 1 to BNL 325 (2nd Ed.)	Recommendations of N. G. Sjöstrand and J. S. Story
$\nu_{235}$	2.43	2.438
$\sigma_a^{235}$	683 $\pm$ 3	680.5 $\pm$ 2.9
$\sigma_{fiss}^{235}$	582 $\pm$ 4	579.9 $\pm$ 4
$\sigma_a^{235}/\sigma_{fiss}^{235}$	1.174	1.174
$\nu_{239}$	2.89	2.901
$\sigma_a^{239}$	1028 $\pm$ 8	1026.7 $\pm$ 7.5
$\sigma_{fiss}^{239}$	742 $\pm$ 4	740.6 $\pm$ 5.5
$\sigma_a^{239}/\sigma_{fiss}^{239}$	1.385	1.386
$\sigma_{fiss}^{239}/\sigma_{fiss}^{235}$	1.275	1.277

sections given in supplement No. 1 to BNL 325 (2nd edition). The cross-section library used with the 40-group Carlson calculations to give the  $U^{235}$  and  $Pu^{235}$  reaction rates was based on values due to Mrs. H. M. Sumner. TERRY [20] gives a 42-group set of cross-sections based on the same fundamental curves as the 40-group set used in this Report. These values are normalized to give the 2200 m/s cross-sections recommended by N-G. Sjöstrand and J. S. Story. A comparison of the 2200 m/s cross-sections is given in Table XXXIII. These are the main objectives in this report:

- (a) The best estimates of reactivity and reaction rates are required for comparison with experiment;
- (b) The errors inherent in the theoretical model of the 5-group scheme need to be revealed;
- (c) It is to be expected that the results of this analysis will be used to appraise the survey calculations made with the existing 5-group programmes.

In order to realize the second of these objectives, the ARISTOS/SANDPIPER values would have to be corrected for the differences between the SANDPIPER and DSN programme libraries. To realize the third objective the values should not be corrected. The major difference between the two sets of data is in the values of  $\nu_{235}$ . As ARISTOS prints the 2-group parameters this correction is easily applied, the ARISTOS and 5-group Carlson values of  $(\eta)_t$  were multiplied by a ratio 2.438/2.43; this correction, which has been made to all the values quoted in this report, raises the reactivities by approximately 0.3%. If one requires the original ARISTOS values it is a simple matter to divide the values of  $(\eta)_t$  given in the text by 1.0030. The differences due to the values of the absorption and fission cross-sections of  $U^{235}$  are not so easily corrected. If the cross-sections in the two libraries both had the same variation with respect to energy, then the difference in magnitude, registered by the 2200-m/s values, would change the reactivities by approximately 0.1%. This is a small correction compared to the differences in reactivity between the two-thermal-group model and the forty-group Carlson model. There are also small differences in the variation of cross-section with energy which introduce uncertainties. In the circumstances, therefore, it was decided to make no correction for the cross-section differences.

The similarity of the ratios of the 2200-m/s fission cross-sections of  $\text{Pu}^{239}$  and  $\text{U}^{235}$  indicate that a direct comparison of the different theoretical values of these fission ratios is justified. The same plutonium cross-sections are used in the two libraries.

### COMPARISON OF ENERGY DISTRIBUTION OF $\text{U}^{235}$ AND $\text{Pu}^{239}$ CROSS-SECTIONS USED IN THE SANDPIPER AND THE D. S. N. LIBRARIES

The following comparison in Tables XXXIV and XXXV shows the discrepancies in the energy variations of the cross-sections with energy. For the purpose of this comparison the SANDPIPER library values were renormalized so that the 2200 m/s are the same as the D. S. N. values. The tabulation was made by Mrs. H. M. Sumner.

TABLE XXXIV

#### $\text{Pu}^{239}$ CROSS-SECTIONS

E (eV)	$\sigma_{a\ 239} \sqrt{E}$		$\sigma_{\text{fiss}\ 239} \sqrt{E}$	
	SANDPIPER (renormalized)	D. S. N.	SANDPIPER (renormalized)	D. S. N.
0	155.5	155.2	113.8	114.9
0.025	163.1	162.8	117.8	117.4
0.050	177.2	173.8	121.7	123.3
0.10	226.8	223.8	146.1	147.9
0.15	335.7	334.6	195.6	206.6
0.20	654.2	641.2	371.2	382.3
0.25	1658.9	1579.0	932.9	928.2
0.27	2399.0	2257.1	1354.4	1327.5
0.28	2736.5	2599.7	1565.0	1527.1
0.29	2957.3	2856.4	1745.7	1676.8
0.30	3017.2	2896.3	1750.7	1691.8
0.32	2509.8	2367.0	1374.4	1394.3
0.35	1398.2	1438.2	857.7	853.4
0.40	652.5	639.2	381.2	384.3
0.45	329.4	334.6	200.6	205.1
0.50	220.3	209.7	125.4	130.8
0.60	127.7	111.9	70.3	72.5

TABLE XXXV

 $U^{235}$  CROSS-SECTIONS

E (eV)	$\sigma_{a 235} \sqrt{E}$		$\sigma_{fiss 235} \sqrt{E}$	
	SANDPIPER (renormalized)	D. S. N	SANDPIPER (renormalized)	D. S. N.
0	116.8	116.0	103.4	98.6
0.025	108.3	108.3	92.4	92.3
0.050	102.2	101.8	86.7	86.8
0.10	93.1	93.0	79.1	79.0
0.15	89.7	90.8	75.3	75.8
0.20	95.7	95.6	78.4	78.2
0.25	115.3	115.6	92.0	92.2
0.27	125.2	125.0	99.1	99.8
0.29	130.8	128.5	103.8	103.1
0.31	127.7	124.9	103.0	102.0
0.35	104.7	103.3	87.5	86.7
0.40	83.8	84.7	72.4	72.1
0.50	67.1	66.1	58.7	57.3
0.60	58.1	58.0	50.7	50.7

## REFERENCES

- [1] HYDER, McK. H. R. and HILBORN, J. W., The Pressure Tube Heavy Water Experiment in DIMPLE, AEEW-R 238.
- [2] ALPIAR, R. A., SANDPIPER III, a programme to calculate 5-group constants for liquid-moderated pressure tube reactors, AEEW-R 92.
- [3] LESLIE, D. C., NEWMARCH, D. A. and BROWN, H. M., ARISTOS - a five group diffusion theory programme for physics calculations on pressure tube reactors, AEEW-R 93.
- [4] AMSTER, H. J., A compendium of thermal neutron cross-sections averaged over the spectra of Wigner and Wilkins, WAPD-185.
- [5] ALLEN, F. R., HICKS, D. and LESLIE, D. C., A five group scheme for P. T. H. W. physics calculations, AEEW-R 105.
- [6] CLARK, H. K., Calculation of high energy events in thermal reactors, DP-609.
- [7] BENOIST, P., Formulation Générale et Calcul Pratique du Coefficient de Diffusion dans un Réseau Comportant des Cavités, CEA 1354.
- [8] HELLSTRAND, C., Measurements of the effective resonance integral in uranium metal and oxide in different geometries, J. appl. Phy. 28 (1957) 1493.
- [9] BANNISTER, G. W. and PULL, I. C., MOCUP. (A report to be issued).
- [10] COHEN, E. R., The thermal neutron flux in a square lattice cell, Nucl. Sci. Engng 1 (1956) 268-279.
- [11] ROBERGE, J. P. and SAILOR, V. L., Parameters of the  $Lu^{176}$  neutron resonance at 0.142 eV, Nucl. Sci. Engng 7 (1960) 502-504.

